Summer 2020

Fast asymptotic algorithm for real-time analysis of multivariate systems and signals by directed transfer function and partial directed coherence measures of connectivity

Farnaz Rezaei

FAST ASYMPTOTIC ALGORITHM FOR REAL-TIME ANALYSIS OF MULTIVARIATE SYSTEMS AND SIGNALS BY DIRECTED TRANSFER FUNCTION AND PARTIAL DIRECTED COHERENCE MEASURES OF CONNECTIVITY

by

Farnaz Rezaei, M.S.

A Thesis Presented in Partial Fulfillment
of the Requirements of the Degree
Master of Science

COLLEGE OF ENGINEERING AND SCIENCE
LOUISIANA TECH UNIVERSITY

May 2020

LOUISIANA TECH UNIVERSITY

THE GRADUATE SCHOOL

_____
Date

We hereby recommend that the thesis prepared under our supervision by

Farnaz Rezaei, M.S.

entitled **Fast asymptotic algorithm for real-time analysis of multivariate systems and signals by directed transfer function and partial directed coherence measures of connectivity**

be accepted in partial fulfillment of the requirements for the Degree of

Master of Science in Mathematics

_____
Supervisor of Thesis Research

_____
Head of Department

_____
Department

Recommendation concurred in:

_____

_____ Advisory Committee

_____

_____

Approved: **Approved**:

_____ _____
Director of Graduate Studies Dean of the Graduate School

_____
Dean of the College

GS Form 13
(8/10)

ABSTRACT

Connectivity Granger-causality measures in the frequency domain, such as the Directed Transfer Function (DTF) and Partial Directed Coherence (PDC) and their variants, constitute a family ϕ of measures that stem from the modeling of multidimensional time series by multivariate autoregressive (MVAR) models. ϕ measures have become popular for evaluation of causal interactions in neuronal networks. Surrogate and asymptotic statistical analysis are the two most frequently used methods to quantify the statistical significance of the derived interactions, a critical step for validation of the results. Each method has its own pros and cons, with the recently published asymptotic methodology being faster. The state-of-the-art asymptotic methods, introduced by Baccala et al., run fairly fast on low-dimensional datasets but become impractical for high-dimensional datasets due to the involved computational time and memory demand; the amount of calculations increases exponentially with the number of time series to be analyzed. This is a huge limitation in the application of ϕ measures to fields that deal with a large number of concurrently acquired time series from probing of complex systems such as the human brain. In this study, we optimized the original algorithms for fast asymptotic analysis of ϕ measures and achieved a reduction of their computation speed by at least three orders of magnitude, thus allowing computation of connectivity measures and their significance in real-time from a plurality of concurrently recorded biological signals. The optimizations were accomplished by a decrease of the

dimension of the involved matrices, reduction of the calculation time of complex functions (e.g. eigenvalue estimation and Cholesky factorization), and variable separation. The superior performance of the proposed optimized algorithms in the estimation of the statistical significance and confidence interval of ϕ measures of causal interactions is shown with simulation examples.

APPROVAL FOR SCHOLARLY DISSEMINATION

The author grants to the Prescott Memorial Library of Louisiana Tech University the right to reproduce, by appropriate methods, upon request, any or all portions of this Thesis. It is understood that "proper request" consists of the agreement, on the part of the requesting party, that said reproduction is for his personal use and that subsequent reproduction will not occur without written approval of the author of this Thesis. Further, any portions of the Thesis used in books, papers, and other works must be appropriately referenced to this Thesis.

Finally, the author of this Thesis reserves the right to publish freely, in the literature, at any time, any or all portions of this Thesis.

Author _____

Date _____

DEDICATION

TABLE OF CONTENTS

ABSTRACT iii

APPROVAL FOR SCHOLARLY DISSEMINATION v

DEDICATION vi

LIST OF FIGURES ix

LIST OF TABLES xi

ACKNOWLEDGMENTS xii

CHAPTER 1 INTRODUCTION 1

CHAPTER 2 BACKGROUND 8

2.1 MVAR Model and its Resultant Connectivity Measures 8

2.1.1 Connectivity Measures of Group γ 9

2.1.2 Connectivity Measures of Group π 12

2.2 Asymptotic Properties of the MVAR Model 15

2.3 Asymptotic Properties of Σe: 17

2.4 Delta Method 18

2.5 Asymptotic Properties of Connectivity Measures 19

CHAPTER 3 FAST ASYMPTOTIC ALGORITHM 25

3.1 Statistical Properties of the Variables 25

3.1.1 Statistical Properties of $\boldsymbol{A}$ 26

3.1.2 Statistical Properties of B 26

3.1.3 Statistical Properties of H 27

3.1.4 Statistical Properties of Σe 28

3.2 Statistical Properties of Connectivity Measures 28

3.2.1 Asymptotic Distribution in Non-Null Case 29

3.2.2 Asymptotic Distribution in Null Case 41

3.3 Computational Complexity of Fast Asymptotic Algorithm 46

CHAPTER 4 PERFORMANCE EVALUATION OF THE PROPOSED FAST ASYMPTOTIC METHODOLOGY 48

4.1 Validation of the Fast Asymptotic Algorithm 48

4.2 Use of Asymptotic Versus Surrogate Statistics 50

4.3 Computation Time of the Fast Versus the Original Asymptotic Algorithm 51

CHAPTER 5 CONCLUSION AND FUTURE WORK 56

5.1 Conclusion 56

5.2 Future Work 58

APPENDIX A MATRIX PROPERTIES 59

A.1 Vectorization Operator (vec) 59

A.2 Rank of Matrix ($rank$) 60

A.3 Moore-Penrose Pseudo-inverse 60

A.4 Commutation Matrix 60

A.5 Kronecker Product Properties: 61

A.6 Spectral Decomposition of a Hermitian Matrix 61

APPENDIX B COMPLEXITY OF THE IMPLEMENTED FUNCTIONS 62

B.1 Matrix Multiplication and Inversion 62

B.2 Cholesky Decomposition 62

B.3 Eigen-pair Calculation 63

BIBLIOGRAPHY 64

LIST OF FIGURES

Figure 4-1: Connectivity diagram between all structures for **Eq. 4-1**. 49

Figure 4-2: Comparative statistics from the original and the new asymptotic estimation of the iPDC(f) connectivity measures for **Eq. 4-1**. The statistical threshold is denoted by black dashed lines if estimated by the original algorithm, and with green triangle symbols if estimated by the new algorithm. The 99% confidence interval is denoted by error bars, gray for the original, and blue for the proposed algorithms. Indexes i and j are denoting the sinks and sources, respectively. 49

Figure 4-3: Comparative statistics from the original and the new asymptotic estimation of the iDTF(f) measures for **Eq. 4-1** . The statistical threshold is denoted by black dashed lines if estimated by the original algorithm, and with green triangle symbols if estimated by the new algorithm. The 99% confidence interval is denoted by error bars, gray for the original, and blue for the proposed algorithms. Indexes i and j are denoting the sinks and sources, respectively..... 50

Figure 4-4: The connectivity measure $|\text{iDTF}|^2$ estimated from signals generated by the simulation example **Eq. 4-1** and its statistical 99% thresholds over frequency obtained by a) the CFT method and 100 surrogates (dashed red lines) and b) by the new asymptotic theory (blue dotted lines). The asymptotic methods provide more accurate statistically significant values for the actual connectivities than the surrogate method. Note: The threshold values with the new are the same as with the original asymptotic theory (see **Figure 4-3**). 51

Figure 4-5: Computation time (min) of "iDTF" (top panels) and "iPDC" (bottom panels) of the original algorithm (blue asterisk *) and the proposed algorithm (red circle o) versus K (left) for $p = 3$, and versus p (right) for $K = 15$. The algorithms were applied to EEG datasets of 10 sec in duration ($fs = 500$ Hz) and iDTF and iPDC were estimated at a single frequency ($f = 41$ Hz). 52

Figure 4-6: Computation time (min) for estimation of the statistics of connectivity measures versus K and p. *Left panel:* Computation time of all measures versus K with $p = 3$ [PDC (diamond), gPDC (dotted lines), iPDC (green asterisk), DTF (circle), gDTF (dashed line), and iDTF (blue asterisk)]. *Right panel:* Computation time versus p with $K = 15$ for iPDC (circle) and iDTF (asterisk). $fs = 2000$ Hz and $f = 41$ Hz. Runtimes of the connectivity measures as functions of K are very similar within group π or group γ; they are almost identical across groups with respect to p..... 53

Figure 4-7: Log of computation time (min) of iPDC (circle) and iDTF(asterisk) versus natural logarithm of K (left) for $p = 3$, and versus natural logarithm of p (right) for $K = 15$. The dashed lines are fitted on curves for $K > 340$ with the approximate slope of 2.7 (left graph), and for $p > 240$ with the approximate slope of 2.03 (right graph). The shaded area represents the minimum slope of 2 and the maximum slope of 3. The algorithms were applied to EEG datasets of 10 sec in duration ($fs = 2000$ Hz) and iDTF and iPDC were estimated at a single frequency ($f = 41$ Hz). 54

Figure 4-8: Computation time (min) of iPDC (circle) and iDTF(asterisk) as a function of number of frequencies the measures are estimated at. The algorithm was applied to 10 sec EEG datasets of a patient with 122 electrodes ($K = 122$), where the model order $p = 8$ was determined using Akaike's information criterion. The dotted lines (blue for iPDC and pink for iDTF) represent the expected computation time when the algorithm runs for each single frequency..... 55

LIST OF TABLES

Table 2-1: Definition of numerator and denominator of ϕ family of **Eq. 2-11** 15

Table 2-2: The terms of the covariance of ϕ family, as explained in **Eq. 2-34** 23

Table 2-3: Dimensions of the variables defined in **Table 2-2** 24

Table 3-1: Variables T_n and T_d for groups of connectivity 35

Table 3-2: Variables S_n and S_d for connectivity measures 35

Table 3-3: Defining variables T_1, T_2, and T_3 in **Eq. 3-54** 38

Table 3-4: Defining variables T_1, T_2, and T_3 for estimating $\Omega_{\phi\sigma}$ in **Eq. 3-37** and **Eq. 3-63** 40

Table 3-5: Time complexity of the Fast Asymptotic algorithm 47

ACKNOWLEDGMENTS

CHAPTER 1

INTRODUCTION

Analysis of multivariate (MV) time series collected from dynamical systems is widely implemented for the study of systems connectivity. The two main connectivity approaches are measuring of coupling, reflecting the presence of interactions, and causality, reflecting driver-response relationships between pairs of series in the MV data set. Causality is interpreted in the context of directional information transfer, whereas coupling evaluates non-directional exchange of information and accounts for the existence of both forward and backward interactions [1, 2]. In the context of "brain connectivity", coupling and causality are typically referred to as "functional" and "effective" connectivity respectively. Thus, while "functional" connectivity indicates the existence of dependencies among brain sites, "effective" connectivity also takes into account their directional interdependencies. Measures of functional and effective connectivity have been developed using linear and nonlinear methods [1, 3].

Formulations of linear connectivity measures derived from multivariate autoregressive (MVAR) analysis of multivariate time series have been introduced in recent years. The spectral signature of the developed MVAR models is used to provide measures of interactions among the time series at specific frequency components [1]. These measures are extensively used to analyze physiological systems, especially to quantify interactions between specific oscillatory components of the brain's electrical

signals such as electroencephalograms (EEG) and magnetic signals such as magnetoencephalograms (MEG) [4, 5]. MVAR analysis of the estimated spectral connectivities of a densely interconnected multivariate (MV) system such as the brain contributes to the understanding of the neurophysiological mechanisms underlying the communication between areas of the brain with oscillatory behavior at particular frequencies, and also in assessing the mechanism of impairment of their communication in pathological conditions [1]. A few current examples of the applications of this analysis to brain disorders include epilepsy (e.g. epileptogenic focus localization), sleep and cognition abnormalities, Parkinson's and Alzheimer's diseases [2, 6-13].

W. J. Granger defined causality by including the following two main criteria in a probabilistic formulation of his analysis of time series [14]: "If event X *causes* event Y, then: (i) event Y (i.e. the *effect*) should occur later than event X, and (ii) the likelihood for occurrence of Y given X is greater than the likelihood of Y without occurrence of X". Thus, the time series X *Granger-causes* time series Y implies that past values of X contain information and can be used for prediction of future values of Y [15]. Two main groups of connectivity quantifiers derived from MVAR, the Directed Transfer Function (DTF) (group γ) and Partial Directed Coherence (PDC) (group π) rely on the concept of Granger-causality and are herein referred to as the ϕ family measures of connectivity [16-18].

Group γ and π measures can provide the direction of connectivities, whether they are cascaded (i.e. direct or indirect) in the case of γ measures, or only partial (direct) in the case of π measures. Modified connectivity measures (*generalized γ and π measures*) have been developed to account for the existence of different scaling across time series

by proper normalization. Model-free connectivity measures (information γ and π measures) have also been developed based on information theory ([16, 19, 20]. Details about the characteristics of the members of the ϕ family measures and their relations are provided in chapter two.

MVAR modeling allows not only the estimation of the strength and direction of the interaction but also statistical tests of their significance [18]. Providing statistical tests of the estimated connectivity measures is a critical component of network analysis. Practical estimation problems, such as random correlation between signals, affect the estimation of MVAR coefficients and subsequently the validity of the connectivity measures that are derived from them [1, 21, 22].

Statistical tests employ the null hypothesis of absence of connectivity and can theoretically detect the true interaction between two signals at a specified level (threshold) of significance. Parametric (model-based, data allow the use of known probability distributions) and nonparametric (not model-based, no need for conditions to be satisfied for use of a known distribution) approaches are the two main techniques employed to test the null hypothesis based on the sampling distribution of connectivities resulting from the use of the connectivity measures [23].

Resampling nonparametric methods such as bootstrapping, jackknife, half-sampling, subsampling, leave-one-out method (LOOM), do not need any prior assumption about data distributions. The basic idea is to estimate the standard error and distribution of the estimator by drawing sufficiently large number of samples. Having mean and standard error of the estimated connectivity measures, several statistical tests,

such as t-test under the assumption of Gaussian distribution, can be applied to characterize their uncertainty [22, 24-26].

Surrogate methods are also nonparametric techniques but construct a large number of new datasets from the original datasets that possess all properties of the original datasets except the one property under statistical investigation. Then, connectivity measures are estimated for the constructed data sets as well as the original data set. The statistically significant connectivity measures are then determined in comparison with the connectivity measures from the surrogate series by performing statistical tests [27]. Such a developed surrogate method, called causal Fourier transform shuffling (CFT), has been developed by Faes et al, 2010 [28] for the ϕ family connectivity measures.

Fourier transform (FT) and amplitude adjusted Fourier transform (AAFT) techniques are nonparametric surrogate methods that preserve the linear behavior (by preserving the power spectrum and autocorrelation of the original datasets) in the constructed surrogate datasets while destroying any nonlinear behavior by randomizing the phase derived from the FT of the original datasets [27]. These FT-based methods were first introduced to test the null hypothesis of linearity of time series, and have also been performed for assessment of the coherence, PDC, and DTF in multivariate processes [17, 29, 30]. In the multivariate FT surrogates investigating the null hypothesis that the data is a realization of a linear multivariate Gaussian process, the cross-spectrum between signals should be preserved in addition to the autocorrelation of each signal. The computational burden for multivariate surrogate analysis and CFT shuffling increases exponentially with the number of datasets (dimension) to be analyzed [21, 27, 28].

While nonparametric statistical approaches are more general, with limited assumptions about the nature of the original datasets, they face limited application to practical problems compared to ones by parametric approaches due to the computational costs involved. Even though the computational cost of sophisticated parametric approaches could make them a good choice in real-time applications, where the dataset size is small or where it is difficult to derive the asymptotic distribution, estimated connectivity measures should be justified by empirical methods[21, 22].

The performance of the derived distribution of measures (e.g. connectivity measures) depends on signal-to-noise ratio (SNR), length and scale variability of the data, as well as the number of constructed shuffled datasets. For example, it has been shown that noise in the data leads to an increase in the statistical threshold and thus, a high rate of false negatives. In this case, in a connectivity analysis, weak connections are more probable to be erroneously discarded. Although increasing the number of datasets improves the false negatives by reducing the threshold, it may produce large number of false positives [21]. In the case of high scale (amplitude) variations in the data, different normalizations of connectivity measures increase the number of false positives of significant connectivity by statistical nonparametric approaches. The number of constructed surrogate datasets should be large to provide reliable assessments. For example, it is recommended that the starting point for the number of surrogates to be at least 100, and it should increase based on the spread of surrogate statistics [27]. For all the above reasons, the computational cost of the empirical (nonparametric) methods limits their applications, especially in the case of high-dimensional datasets, like EEG or MEG signals that involve recorded signals from hundreds of brain sites [21].

When the exact statistical distribution of an estimator is difficult to obtain, we rely on its asymptotic distribution, that is, the distribution approximated based on the properties of statistics from large datasets. In parametric statistical approaches, the asymptotic properties of a continuous and differentiable function of a random variable (e.g. a measure of connectivity) can be obtained by performing the *delta method* that consists of Taylor series expansion and Slutsky's theorem [31]. The asymptotic parametric approach makes all different connectivity formulations independent of applied normalization and thus the statistical testing for actual connectivities more robust [21]. It has also been shown that asymptotic approaches, based on the analytical estimation of the statistical distributions of the estimators, provide almost identical assessments like the ones from empirical approaches [21].

The asymptotic properties of PDC under the null hypothesis were examined by Schelter et al. in 2006 [32] and later completed in terms of both null and non-null cases by Takahashi et al. in 2007 [33]. In 2013 and 2016, Baccala et al. analytically derived the asymptotic behavior of all the different forms of π and γ [34, 35]. They demonstrated that the squared ϕ estimators asymptotically converge to χ^2 distribution in the null case and to a Gaussian distribution in the non-null case.

The methods developed by Baccala are the state-of-the-art in this area and are currently included in the "unified asymptotic MATLAB toolbox". They are herein first reviewed and then further optimized. A major disadvantage of the current unified asymptotic approach is the time required for calculation of the statistics of the estimated measures, which increases also exponentially with the dimension of the employed models

that fit the data (e.g. number of EEG signals). Nowadays, multichannel EEG is performed with 100 to 200 sensors (electrodes), and MEG with 200 to 300 sensors, over hours. Therefore, the current algorithms in the unified asymptotic toolbox cannot be practically applied to multivariate analysis of such multivariate EEG or MEG recorded signals towards an effective brain network analysis [36].

In this study, we first review the existing formulation of the unified asymptotic statistics (**chapter two**) and then propose a new, much faster, asymptotic statistical analysis, which employs successive decomposition of the time-consuming processes by special matrix manipulation techniques and separation of variables methodology. The mathematical details related to this novel methodology are provided in **chapter three** and a sequence of appendices (**Appendix A1 to A6** and **Appendix B1 to B3**). These optimization procedures result in orders of magnitude of faster algorithms that can deal, in close to real-time, with derivations of the asymptotic statistics of the estimated connectivity measures from 100+ dimensional data series.

Validation of the proposed algorithms was accomplished in a reported in the literature exemplary simulation system. The results from this validation are presented in **chapter four,** and the derived overall conclusions from this study and suggestions for future work in **chapter five**.

CHAPTER 2

BACKGROUND

The objective of this chapter is to provide an overview of the Multivariate Autoregressive (MVAR) process, and some common connectivity measures we focused on in this study. The asymptotic properties of these connectivity quantifiers noted as ϕ measures are reviewed, and the original unified asymptotic algorithm introduced by Baccala et al. [34, 35] and its disadvantage are discussed.

2.1 MVAR Model and its Resultant Connectivity Measures

One of the most common tools in MV time series analysis is the multivariate autoregressive (MVAR) model. Let $\boldsymbol{y}(n) = [y_1(n), y_2(n), \mathrm{y}(n), \dots, y_K(n)]^T$ be a K-dimensional vector at time $n = t \times f_s$, where f_s is the sampling frequency of the data, and with its components being zero mean time series, $y_i(n)$. Then, a K-dimensional autoregressive (MVAR) model of order p, where each present value $\boldsymbol{y}(n)$ depends on p past values of the observed time series is constructed as:

$$\boldsymbol{y}(n) = \sum_{\tau=1}^{p} A(\tau)\boldsymbol{y}(n-\tau) + \boldsymbol{\epsilon}(n) \qquad \textbf{Eq. 2-1}$$

p may be determined using criteria developed in the framework of information theory, and $A(\tau)$ is the model's $K \times K$ coefficient matrix (i.e. model parameters) at lag τ

, $(\tau = 1, \dots, p)$ estimated through minimization of the residual noise $\boldsymbol{\epsilon}(n)$. If the model fits the data well, the noise (innovation) vector $\boldsymbol{\epsilon}(n) = [\epsilon_1(\mathrm{n}), \cdots, \epsilon_K(n)]^T$ follows an MV standard white noise process, assuming that each vector component $y_i(n)$ is at least weakly stationary time series.

Standard white noise is a continuous process having zero mean, with the correlation matrix equals to zero for each lag $\tau > 0$ and equals to nonsingular covariance $\Sigma_{\mathrm{e}} = \begin{bmatrix} \sigma_{11} & \cdots & \sigma_{1K} \\ \vdots & \ddots & \vdots \\ \sigma_{K1} & \cdots & \sigma_{KK} \end{bmatrix}$ for $\tau = 0$.

The spectral representation of **Eq. 2-1** is widely used in derivation of connectivity measures defined in the next sections:

$$\left(I_K - \sum_{\tau=1}^{p} A(\tau) e^{-j2\pi f \tau}\right) \boldsymbol{y}(f) = E(f) \qquad \textbf{Eq. 2-2}$$

where I_K is the $K \times K$ identity matrix, and $E(f)$ is the residual noise. If $B(f) = I_K - \sum_{\tau=1}^{p} A(\tau) e^{-j2\pi f \tau}$, then $B(f)$ essentially results from the Fourier transform of the augmented matrix A of the coefficients of the model (setting $A(0) = I_K$), and for this reason, we refer to it as the coefficient matrix B in the rest of this study.

Various forms of frequency-domain connectivity measures, family of $\boldsymbol{\phi}$, were derived from **Eq. 2-2**. $\boldsymbol{\phi}$ family is categorized into two main groups: group γ extracted from coherence, and group π extracted from partial coherence. A brief review of $\boldsymbol{\phi}$ family is discussed in the following sections.

2.1.1 Connectivity Measures of Group γ

MVAR defined in **Eq. 2-1** is the common representation of the MV closed-loop process for time series analysis. In signal processing framework, $\boldsymbol{y}(n)$ and $\boldsymbol{\epsilon}(n)$ are

respectively the output and input of the linear time-invariant filter with the impulse response matrix $H(k)$:

$$\boldsymbol{y}(n) = \sum_{k=-\infty}^{\infty} H(k)\boldsymbol{\epsilon}(n-k) \qquad \textbf{Eq. 2-3}$$

Converting into the frequency domain, $\boldsymbol{y}(f)$ can be obtained by finding the Fourier transform of **Eq. 2-3**:

$$\boldsymbol{y}(f) = H(f)\,\mathrm{E}(f) \qquad \textbf{Eq. 2-4}$$

where $H(f)$ is the transfer function matrix. Comparing **Eq. 2-4** and **Eq. 2-2**, we can conclude that $H(f) = B^{-1}(f)$. The spectral density matrix of the process can be factored uniquely as:

$$S(f) = \boldsymbol{y}(f)\boldsymbol{y}(f)^{\mathrm{H}} = H(f)\,\mathrm{E}(f)\,\mathrm{E}(f)^{H}\,H(f)^{H} = H(f)\Sigma_e H^{\mathrm{H}}(f) \qquad \textbf{Eq. 2-5}$$

Under the assumption of strict causality meaning that $\boldsymbol{\epsilon}(n)$ is uncorrelated even at $\tau = 0$, the covariance Σ_e is diagonal:

$$S_{ij}(f) = \sum_{m=1}^{K} \sigma_{\mathrm{mm}} H_{im}(f)\,H^{*}{}_{jm}(f) \qquad \textbf{Eq. 2-6}$$

Considering the definition of ordinary coherence (Coh) which explains the simultaneous interaction between signals, and by applying **Eq. 2-6**, the decomposition of Coh equation is:

$$Coh_{ij}(f) = \frac{S_{ij}(f)}{\sqrt{S_{ii}(f)S_{jj}(f)}}$$

$$= \sum_{m=1}^{K} \frac{\sigma_{\mathrm{mm}}{}^{\frac{1}{2}} H_{im}(f)}{\sqrt{S_{ii}(f)}} \frac{\sigma_{\mathrm{mm}}{}^{\frac{1}{2}} H^{*}{}_{jm}(f)}{\sqrt{S_{jj}(f)}} \qquad \textbf{Eq. 2-7}$$

$$= \sum_{m=1}^{K} \gamma_{im}(f)\, \gamma_{jm}{}^{*}(f)$$

Where $S_{ii}(f) = \sum_{m=1}^{K} \sigma_{\mathrm{mm}} |H_{im}(f)|^2$. Hence, in **Eq. 2-7** the normalization was performed with respect to the receiver structure. Thus, in the $j \rightarrow i$ interaction, $\gamma_{ij}(f)$ emphasizes the effect of the outflow from the source j to the sink i, and is therefore considered a better measure of the effect of the outflow from the source j to the sink i.

$\gamma_{ij}(f)$ stemming as a direct factor from the decomposition of coherence (**Eq. 2-7**) is named Generalized directed transfer function ($gDTF$). The $gDTF$ was originally introduced by Akaike in 1968 as the noise contribution ratio (NCR) [37]. Then, Saito and Harashima in 1981 reformulated it as a bivariate spectral connectivity measure of feed-forward and feed-backward processes and named it Directed Coherence (DC) [38]. It was further developed as an MV connectivity measure using the MVAR model by Baccala in 1998 [39].

For the particular case, where Σ_e is assumed to be an identity matrix, $\sigma_{mm} = 1$ for all $m = 1,2, \dots, K$, $\gamma_{ij}(f)$ in **Eq. 2-7** represents a connectivity measure named directed transfer function (DTF) which was proposed by Kaminski and Blinowska [19]. To make this assumption, Kaminski rescaled the original data into a data set with zero mean and unitary variance. However, it was shown in [40] that in the case of high variability of σ_{mm} , DTF may falsely detect the causality.

Solving the scale invariance problem by renormalization of innovation covariance matrix to a unitary matrix is done in $gDTF$, and thus improves the causality estimation.

Also, to quantify the absolute scale-invariant connectivity strength, information DTF ($iDTF$) was introduced by Takahashi et al. as the coherence between the time series $\boldsymbol{y}(n)$ and partialized innovation process ($\varpi(n)$), where $iDTF_{j\to i} = Coh_{x_i\varpi_j}(f)$ [41].

Although coherence is a coupling measure, $\gamma_{ij}(f)$ is a measure of causality (according to **Eq. 2-7**, the existence of any significant path between y_j and y_i leads to the causality from y_j to y_i). In other words, $\gamma(f)$ is an asymmetric factor extracted from the symmetric connectivity measures [1].

Moreover, $H_{ij}(f)$ as the inverse of $B(f)$ includes cascading terms which represent many possible alternative paths connecting j to i. As a result, group γ contains both direct and indirect causal effects [1].

2.1.2 Connectivity Measures of Group π

By analogy with DTF, PDC is derived from the decomposition of partial coherence ($PCoh$). Partial coherence describes the mutual interaction between two time series after eliminating the influence of all other simultaneously observed time series. Combining the element of inverse spectral matrix ($P(f)$) with the aim of normalization, $PCoh$ is calculated as:

$$PCoh_{ij}(f) = -\frac{P_{ij}(f)}{\sqrt{P_{ii}(f)P_{jj}(f)}} \qquad \textbf{Eq. 2-8}$$

The inverse of **Eq. 2-5** results in:

$$P(f) = H^{-H}(f){\Sigma_e}^{-1}H^{-1}(f) = B^H(f){\Sigma_e}^{-1}\mathrm{B}(f) \qquad \textbf{Eq. 2-9}$$

Substituting **Eq. 2-9** in **Eq. 2-8**, $PCoh$ is decomposed into two directed partial coherences. Assuming strict causality:

$$PCoh_{ij}(f) = -\sum_{m=1}^{K} \frac{\sigma_{\mathrm{mm}}{}^{-\frac{1}{2}} B_{mj}(f)}{\sqrt{P_{jj}(f)}} \frac{\sigma_{\mathrm{mm}}{}^{-\frac{1}{2}} B^{*}{}_{mi}(f)}{\sqrt{P_{ii}(f)}} = -\sum_{m=1}^{K} \pi_{mj}(f)\, \pi_{mi}{}^{*}(f) \qquad \textbf{Eq. 2-10}$$

Where $P_{jj}(f) = \sum_{m=1}^{K} \sigma_{\mathrm{mm}}{}^{-1} \left|B_{mj}(f)\right|^2$. According to **Eq. 2-10**, in $\pi_{ij}(f)$ the normalization was done with respect to sender structure. Hence, it emphasizes the receiving side of the $j \rightarrow i$ interaction and is therefore considered a better measure of the effect of the inflow to the sink i from the source j in the $j \rightarrow i$ interaction.

$\pi_{ij}(f)$ derived in **Eq. 2-10** named Generalized partial directed coherence ($gPDC$) and was introduced by Baccala et al. in 2007 [42].

Similarly, by assuming that Σ_e is an identity matrix, π_{ij} in **Eq. 2-10** reflects Partial Directed Coherence (PDC) which was proposed by Baccala and Sameshima in 2001 [16]. Improvement of the scale invariance problem of PDC and $gPDC$ was done by defining the information PDC ($iPDC$) introduced by Takahashi et al. in 2010. $iPDC$ relates PDC to information flows in the MVAR formulation [41].

$iPDC$ is derived from the coherence between innovation noise and mutual partialization of the components of the observed signal. Defining η_j as the partialized process associated with y_j, η_j is the residue of the projection of y_j onto the remaining process. $iPDC_{j\rightarrow i}$ equals to the $Coh_{\epsilon_i \eta_j}(f)$, with $S_{\eta_j \eta_j}$ indicating a partial spectrum of y_j given the remaining process. $S_{\eta_j \eta_j}$ is derived through the partitioned matrix inversion formula. According to [41], $S_{\epsilon_i \eta_j} = B_{ij}(f) S_{\eta_j \eta_j}$, $S_{\epsilon_i \epsilon_i} = \sigma_{ii}$, and $S_{\eta_j \eta_j} =$

$\left({B_{:j}}^{H}(f){\Sigma_e}^{-1}B_{:j}(f)\right)^{-1}$, where $B_{:j}(f)$ is a vector containing all the elements of column j of $B(f)$ [41]. The formula for $iPDC$ is provided in **Table 2-1**.

In contrast with group γ, the group π measures directly depend on the coefficient of the model. Therefore, the off-diagonal connectivity pairs in group π are significant whenever its corresponding element in $A(\tau)$ is significant for some τ. This chief property develops an estimator that can inherently distinguish between direct and indirect connections and makes the connectivity quantifiers in group π as a direct causality measure.

Although the directed characteristics of the group π establish the superiority over the group γ, being a factor of an inverse spectral matrix, they lack clear physical explanations (except for $iPDC$ which is derived from coherence) [1, 41].

The squared modulus of ϕ family, $\left|\phi_{ij}(f)\right|^2$, is the commonly real-value format of connectivity measures which indicates the strength of connection. In the rest of this study, the square of connectivity measures was implemented as ϕ family.

Moreover, $\left|\phi_{ij}(f)\right|^2$ can be separated in terms of numerator ($\phi_{n(ij)}$) and denominator ($\phi_{d(ij)}$) as:

$$\left|\phi_{ij}(f)\right|^2 = \frac{\phi_{n(ij)}}{\phi_{d(ij)}} \qquad \textbf{Eq. 2-11}$$

The variables $\phi_{n(ij)}$ and $\phi_{d(ij)}$ for different members of group π and group γ are defined in **Table 2-1**.

Table 2-1: Definition of numerator and denominator of ϕ family of **Eq. 2-11**

$\boldsymbol{\gamma_{j\to i}(f)}$	$\boldsymbol{\gamma_{n(ij)}}$	$\boldsymbol{\gamma_{d(ij)}}$	$\boldsymbol{\pi_{j\to i}(f)}$	$\boldsymbol{\pi_{n(ij)}}$	$\boldsymbol{\pi_{d(ij)}}$
DTF	$\lvert H_{ij}(f)\rvert^2$	$\sum_{m=1}^{K}\lvert H_{im}(f)\rvert^2$	**PDC**	$\lvert B_{ij}(f)\rvert^2$	$\sum_{m=1}^{K}\lvert B_{mj}(f)\rvert^2$
gDTF	$\sigma_{jj}\lvert H_{ij}(f)\rvert^2$	$\sum_{m=1}^{K}\sigma_{mm}\lvert H_{im}(f)\rvert^2$	***gPDC***	$\sigma_{ii}^{-1}\lvert B_{ij}(f)\rvert^2$	$\sum_{m=1}^{K}\sigma_{mm}^{-1}\lvert B_{mj}(f)\rvert^2$
iDTF	$\sigma_{jj}\lvert H_{ij}(f)\rvert^2$	$H_{i:}(f)\Sigma_e H_{i:}^{H}(f)$	***iPDC***	$\sigma_{ii}^{-1}\lvert B_{ij}(f)\rvert^2$	$B_{:j}^{H}(f)\Sigma_e^{-1}B_{:j}(f)$

2.2 Asymptotic Properties of the MVAR Model[43]

The MVAR model in **Eq. 2-1** can be rewritten in the matrix format as:

$$Y = \boldsymbol{A}X + E \qquad \textbf{Eq. 2-12}$$

Where $Y = \big(\boldsymbol{y}(1), \dots\ \boldsymbol{y}(n_s)\big)$ with a sample size of n_s and the dimension of $(K \times n_s)$, $\boldsymbol{A} = [A(1), \dots A(p)]$ with the dimension of $(K \times Kp)$ which is the lagged MVAR(p) coefficient matrix, $X = \big(x_0, \dots, x_{n_s-1}\big)$ with the dimension of $(Kp \times n_s)$, $x_n = [\boldsymbol{y}(n), \dots, \boldsymbol{y}(n-p+1)]^T$ with the dimension of $(Kp \times 1)$, and $E = \big(\boldsymbol{\epsilon}(1), \cdots, \boldsymbol{\epsilon}(n_s)\big)$ is the $(K \times n_s)$ innovation matrix. Also, the vectorization of **Eq. 2-12** can be done as:

$$vec(Y) = vec(\boldsymbol{A}X) + vec(E) = (X^T \otimes I_K)\boldsymbol{a} + vec(E) \qquad \textbf{Eq. 2-13}$$

Where $\boldsymbol{a} = vec(\boldsymbol{A})$, $\otimes$ is the Kronecker product operator, and vec is column stacking operator. The estimation of $\boldsymbol{a}$ is found through the minimalization of the residual noise. Therefore, by applying the multivariate least square (LS) estimation, as the covariance matrix of E is $\big(I_{n_s} \otimes \Sigma_e\big)$, $\widehat{\boldsymbol{a}}$, the estimator of $\boldsymbol{a}$ can be obtained by minimizing **Eq. 2-13**:

$$S(\boldsymbol{a}) = vec(E)^T\left(I_{n_s}\otimes\Sigma_e\right)^{-1}vec(E) = \\ [vec(Y) - (X^T\otimes I_K)\boldsymbol{a}]^T\left(\left(I_{n_s}\otimes{\Sigma_e}^{-1}\right)\right)[vec(Y) - (X^T\otimes I_K)\boldsymbol{a}] \quad \textbf{Eq. 2-14}$$

Applying the Kronecker product properties, $S(\boldsymbol{a})$ can be rewritten as:

$$S(\boldsymbol{a}) = vec(Y)^T\left(I_{n_s}\otimes{\Sigma_e}^{-1}\right)vec(Y) + \\ \boldsymbol{a}^T\left(XX^T\otimes{\Sigma_e}^{-1}\right)\boldsymbol{a} - 2\boldsymbol{a}^T\left(X\otimes{\Sigma_e}^{-1}\right)vec(Y) \quad \textbf{Eq. 2-15}$$

Therefore, the LS estimator $\widehat{\boldsymbol{a}}$, can be achieved by finding the root of the derivative of **Eq. 2-15** with respect to $\boldsymbol{a}$:

$$\frac{\partial S(\boldsymbol{a})}{\partial \boldsymbol{a}} = 2\left(XX^T\otimes{\Sigma_e}^{-1}\right)\boldsymbol{a} - 2\left(X\otimes{\Sigma_e}^{-1}\right)vec(Y) = 0 \quad \textbf{Eq. 2-16}$$

$$\widehat{\boldsymbol{a}} = ((XX^T)^{-1}\otimes\Sigma_e)\left(X\otimes{\Sigma_e}^{-1}\right)vec(Y) = \\ ((XX^T)^{-1}X\otimes \mathrm{I_K})vec(Y) = vec(YX^T(XX^T)^{-1}) \quad \textbf{Eq. 2-17}$$

Thus, $\widehat{\boldsymbol{A}} = YX^T(XX^T)^{-1}$. Also, finding the Hessian of $S(\boldsymbol{a})$ confirms that $\widehat{\boldsymbol{a}}$ is the minimum vector. By substituting **Eq. 2-12**:

$$\widehat{\boldsymbol{A}} = (\boldsymbol{A}X + E)X^T(XX^T)^{-1} = \boldsymbol{A} + EX^T(XX^T)^{-1} \quad \textbf{Eq. 2-18}$$

It is proven in [43] that for $\boldsymbol{y}(n)$ generated by stationary, stable MVAR(p) process, and MV standard white noise residuals $\boldsymbol{\epsilon}(t)$, the followings hold:

$$\Gamma_y = \lim_{n_s\to\infty}\frac{XX^T}{n_s} \text{ exists and it is nonsingular} \\ \frac{1}{\sqrt{n_s}}(EX^T) = \frac{1}{\sqrt{n_s}}(X\otimes I_K)E \xrightarrow{d} \mathcal{N}\left(0, \Gamma_y\otimes\Sigma_{\boldsymbol{e}}\right) \quad \textbf{Eq. 2-19}$$

The consistency of $\widehat{\boldsymbol{A}}$ is found by proving that $\lim_{n_s\to\infty}\left(\widehat{\boldsymbol{A}} - \boldsymbol{A}\right) = 0$. Hence, by applying **Eq. 2-18** and **Eq. 2-19**:

$$\lim_{n_s\to\infty}\left(\widehat{\boldsymbol{A}}-\boldsymbol{A}\right)=\lim_{n_s\to\infty}\boldsymbol{E}X^T(XX^T)^{-1}=$$

$$\lim_{n_s\to\infty}\left(\frac{\boldsymbol{E}X^T}{n_s}\right)\lim_{n_s\to\infty}\left(\frac{XX^T}{n_s}\right)^{-1}=0 \qquad \textbf{Eq. 2-20}$$

Furthermore, the asymptotic behavior of $\widehat{\boldsymbol{A}}$ is established using the vector format of **Eq. 2-18** as:

$$\sqrt{n_s}vec\left(\widehat{\boldsymbol{A}}-\boldsymbol{A}\right)=\sqrt{n_s}(\widehat{\boldsymbol{a}}-\boldsymbol{a})=$$

$$\sqrt{n_s}((XX^T)^{-1}X\otimes I_K)E=\left\{\left(\frac{XX^T}{n_s}\right)^{-1}\otimes I_K\right\}\left\{\frac{1}{\sqrt{n_s}}(X\otimes I_K)E\right\}= \qquad \textbf{Eq. 2-21}$$

$$\left\{{\Gamma_y}^{-1}\otimes I_K\right\}\left\{\frac{1}{\sqrt{n_s}}(X\otimes I_K)E\right\}$$

Substituting **Eq. 2-19** in **Eq. 2-21**, and applying *delta method* (discussed in the next section), the covariance matrix is:

$$\left({\Gamma_y}^{-1}\otimes I_K\right)^T\left(\Gamma_y\otimes\Sigma_{\boldsymbol{e}}\right)\left({\Gamma_y}^{-1}\otimes I_K\right)={\Gamma_y}^{-1}\otimes\Sigma_{\boldsymbol{e}} \qquad \textbf{Eq. 2-22}$$

Therefore, the asymptotic distribution of $\widehat{\boldsymbol{A}}$ can be summarized as:

$$\sqrt{n_s}vec\left(\widehat{\boldsymbol{A}}-\boldsymbol{A}\right)=\sqrt{n_s}(\widehat{\boldsymbol{a}}-\boldsymbol{a})\xrightarrow{d}\mathcal{N}(0,\Omega_{\boldsymbol{a}})$$

$$\Omega_{\boldsymbol{a}}={\Gamma_y}^{-1}\otimes\Sigma_{\boldsymbol{e}} \qquad \textbf{Eq. 2-23}$$

Also, it was shown in [43] that the asymptotic properties of the maximum likelihood estimator are equivalent to the LS estimator.

2.3 Asymptotic Properties of $\boldsymbol{\Sigma_e}$:

As it was proven in reference [43], by defining $\boldsymbol{\sigma}\triangleq vec(\Sigma_e)$, the asymptotic distribution of $\boldsymbol{\sigma}$ is:

$$\sqrt{n_s}(\widehat{\boldsymbol{\sigma}} - \boldsymbol{\sigma}) \xrightarrow{d} \mathcal{N}(0, \Omega_{\boldsymbol{\sigma}})$$

$$\Omega_{\boldsymbol{\sigma}} = 2D_K D_K^{+}(\Sigma_e \otimes \Sigma_e) D_K^{+T} D_K^{T} \qquad \textbf{Eq. 2-24}$$

where D_K^{+} is the Moore-Penrose pseudo-inverse of the standard duplication matrix.

2.4 Delta Method

Let the distribution of $\boldsymbol{u}_n = (u_1, u_2, \dots, u_K)^T$ from n observation converges to:

$$\sqrt{n}(\boldsymbol{u}_n - \boldsymbol{\mu}) \xrightarrow{d} \mathcal{N}(0, \Sigma_u) \qquad \textbf{Eq. 2-25}$$

Suppose $g(\boldsymbol{u})$ is a real-valued, continuously differentiable function at the neighbor of $\boldsymbol{\mu}$, vanishing up to order m about point $\boldsymbol{\mu}$ in Taylor expansion and non-vanishing in the m^{th} term

$$\left(\sqrt{n}\right)^m (\hat{g}(u_n) - g(\mu)) \xrightarrow{d} \frac{1}{m!} \sum_{i_1=1}^{k} \cdots \sum_{i_m=1}^{k} \left. \frac{\partial^m g}{\partial u_{i_1} \dots \partial u_{i_m}} \right|_{\boldsymbol{\mu}} \prod_{j=1}^{m} \boldsymbol{X}_{i_j} \qquad \textbf{Eq. 2-26}$$

with

$$\boldsymbol{X} = (X_1, \dots, X_k)^T \sim \mathcal{N}(0, \Sigma_u) \qquad \textbf{Eq. 2-27}$$

For large n and non-zero first-order derivatives, the following corollary is presumed [31].

Corollary 3.1 for a real differentiable function $g(\boldsymbol{u})$, the first *delta method* approximation is:

$$\sqrt{n}\left(\hat{g}(\boldsymbol{u}_n) - g(\boldsymbol{\mu})\right) \xrightarrow{d} \mathcal{N}(0, \nabla g^T \Sigma_u \nabla g) \qquad \textbf{Eq. 2-28}$$

where ∇g is the gradient of $g(u)$ evaluated at $\boldsymbol{\mu}$.

2.5 Asymptotic Properties of Connectivity Measures

Baccala et al. derived a unified asymptotic property for three major formulations of group π, PDC, $gPDC$, and $iPDC$ [34]. Later, they found the asymptotic statistical characteristics of corresponding connectivity measures in group γ including DTF, $gDTF$, and $iDTF$ [35].

In both studies, the square of ϕ family was examined under the null hypothesis of:

$$H_0 : \left|\phi_{ij}(f)\right|^2 = 0 \qquad \forall\, i,j \in \{1,\dots,K\} \qquad \textbf{Eq. 2-29}$$

Eq. 2-29 explains the absence of connectivity at specific frequency f between the two sites i and j.

For the functions of group π, they concluded that $\left|\pi_{ij}(f)\right|^2$ is a function of variable $\theta = \left[\overline{b}^T, \boldsymbol{\sigma}^T\right]^T$, where $\overline{b}$ was defined as a function of $\boldsymbol{a}$:

$$\overline{b} = \begin{bmatrix} vec(I_{K^2}) \\ vec(0_{K^2}) \end{bmatrix} - (\mathcal{C} \otimes \mathrm{I}_{K^2})\boldsymbol{a} \qquad \textbf{Eq. 2-30}$$

with,

$$\mathcal{C} = \begin{bmatrix} \cos(2\pi f) & \dots & \cos(2\pi fp) \\ -\sin(2\pi f) & \dots & -\sin(2\pi fp) \end{bmatrix}_{2\times p} \qquad \textbf{Eq. 2-31}$$

The estimator $\hat{\theta}$ asymptotically converges to a normal distribution with the covariance of Ω_θ:

$$\Omega_\theta = \begin{bmatrix} \Omega_{\overline{b}} & 0_{2K^2} \\ 0_{K^2} & \Omega_{\boldsymbol{\sigma}} \end{bmatrix} \qquad \textbf{Eq. 2-32}$$

where 0_n is a $(n \times n)$ matrix with all zero entries. By applying the *delta method*, the asymptotic distribution of the estimator $\hat{\overline{b}}$ was obtained as a normal distribution with the covariance $\Omega_{\overline{b}}$:

$$\Omega_{\overline{b}} = (\mathcal{C} \otimes \mathrm{I}_{K^2}) \begin{bmatrix} \Omega_{\boldsymbol{a}} & \Omega_{\boldsymbol{a}} \\ \Omega_{\boldsymbol{a}} & \Omega_{\boldsymbol{a}} \end{bmatrix} (\mathcal{C}^T \otimes \mathrm{I}_{K^2}) \qquad \textbf{Eq. 2-33}$$

Since $\left|\pi_{ij}(f)\right|^2$ is a real-value function of θ with continuous partial derivatives, the covariance of $\left|\hat{\pi}_{ij}(f)\right|^2$ represented by Ω_π for large n_s is:

$$\Omega_\pi = \left(\nabla \left|\pi_{ij}(f)\right|^2\right) \Omega_\theta \left(\nabla \left|\pi_{ij}(f)\right|^2\right)^T =$$

$$\begin{bmatrix} \frac{\partial |\pi_{ij}(f)|^2}{\partial \overline{b}^T} & \frac{\partial |\pi_{ij}(f)|^2}{\partial \boldsymbol{\sigma}^T} \end{bmatrix} \begin{bmatrix} \Omega_{\overline{b}} & 0_{2K^2} \\ 0_{K^2} & \Omega_{\boldsymbol{\sigma}} \end{bmatrix} \begin{bmatrix} \left(\frac{\partial |\pi_{ij}(f)|^2}{\partial \overline{b}^T}\right)^T \\ \left(\frac{\partial |\pi_{ij}(f)|^2}{\partial \boldsymbol{\sigma}^T}\right)^T \end{bmatrix} = \qquad \textbf{Eq. 2-34}$$

$$\left(\nabla_{\overline{b}} \left|\pi_{ij}(f)\right|^2\right) \Omega_{\overline{b}} \left(\nabla_{\overline{b}} \left|\pi_{ij}(f)\right|^2\right)^{\boldsymbol{T}} +$$

$$\left(\nabla_{\boldsymbol{\sigma}} \left|\pi_{ij}(f)\right|^2\right) \Omega_{\boldsymbol{\sigma}} \left(\nabla_{\boldsymbol{\sigma}} \left|\pi_{ij}(f)\right|^2\right)^{\boldsymbol{T}} = \Omega_{\pi_{\overline{b}}} + \Omega_{\pi_{\boldsymbol{\sigma}}}$$

Where $\nabla_x g$ denotes the partial derivative of g with respect to x. The fraction form of $\left|\pi_{ij}(f)\right|^2$ is provided in the reference [34] and with a minor difference, it is similar to what defined in **Table 3-1** and **Table 3-2** of chapter three. The equations of $\nabla_{\overline{b}} \left|\pi_{ij}(f)\right|^2$ and $\nabla_{\boldsymbol{\sigma}} \left|\pi_{ij}(f)\right|^2$ proved in reference [34] are summarized in **Table 2-2**.

In the same fashion, for the members of group γ, $\theta = \left[\overline{h}^T, \boldsymbol{\sigma}^T\right]^T$, where $\overline{h}$ is the vector format of $H(f)$ which is decomposed in terms of real and imaginary parts. According to [35], $\hat{\overline{h}}$ has a normal distribution with the covariance $\Omega_{\overline{h}}$ as:

$$\Omega_{\overline{h}} = \mathcal{H}\,\Omega_{\overline{b}}\,\mathcal{H}^T \qquad \textbf{Eq. 2-35}$$

where,

$$\mathcal{H} = -\begin{bmatrix} Real(H^T(f)\otimes H(f)) & -Imag(H^T(f)\otimes H(f)) \\ Imag(H^T(f)\otimes H(f)) & Real(H^T(f)\otimes H(f)) \end{bmatrix} \qquad \textbf{Eq. 2-36}$$

Applying the *delta method*, the asymptotic distribution of $\left|\hat{\gamma}_{ij}(f)\right|^2$ was obtained in [35]. According to [35], $\left|\hat{\gamma}_{ij}(f)\right|^2$ asymptotically converges to normal distribution whose covariance, Ω_γ can be obtained by replacing $\overline{b}$ with $\overline{h}$ in **Eq. 2-34**, and its variables are defined in **Table 2-2**.

Having the asymptotic distribution of ϕ family, the confidence interval of the estimated connectivity measures has been acquired in the case of rejection of the null hypothesis. However, it is shown in [34, 35] that Gaussianity breaks down when there are no significant connections, in which case the next term in the *delta method* provides the asymptotic distribution for those connections that can be used to construct a rigorous hypothesis test of connectivity.

In the group π, the second-order derivative terms in the right-hand side of the *delta method* are zero except for $\nabla_{\overline{b},\overline{b}}\left|\pi_{ij}(f)\right|^2$ which is $X^T I_{ij}^c(I_{2K}\otimes S_n)I_{ij}^c X/\pi_{d(ij)}$ where $X\sim\mathcal{N}(0,\ \Omega_{\pi_{\overline{b}}})$. Introducing standard normal random variable Z where $= L_{\overline{b}}Z$, and $L_{\overline{b}}$ is a Cholesky factor of $\Omega_{\pi_{\overline{b}}}$:

$$X^T I_{ij}^c(I_{2K}\otimes S_n)I_{ij}^c X = Z^T L_{\overline{b}}^T I_{ij}^c(I_{2K}\otimes S_n)I_{ij}^c L_{\overline{b}} Z = Z^T \boldsymbol{D}_\pi\, Z \qquad \textbf{Eq. 2-37}$$

As $\boldsymbol{D}_\pi$ is Hermitian matrix, spectral decomposition of $\boldsymbol{D}_\pi$ leads to:

$$Z^T \boldsymbol{D}_\pi \, Z = \sum_{k=1}^{q} \lambda_k Z^T v_k v_k^T Z \qquad \textbf{Eq. 2-38}$$

where v_k is the k^{th} eigenvector of $\boldsymbol{D}_\pi$ associated with λ_k. Defining $\xi_k = v_k^T Z$ (ξ_k has standard normal distribution), $Z^T \boldsymbol{D}_\pi \, Z = \sum_{k=1}^{q} \lambda_k {\xi_k}^2$. Similar relationships were obtained for group γ in [35]. Thus, under the null condition, ϕ quantifier represents a linear combination of χ_1^2 distribution whose multiplier was elicited from $\phi_{n(ij)}(f)$.

The computational steps for justifying the connectivity measures $\left|\phi_{ij}(f)\right|^2$, for pair $(i,j) : i,j \in \{1,\dots,K\}$ and at specific frequency f are summarized below. These steps consist of finding the threshold in the null case and confidence interval in the non-null case.

1. Calculating a $(2K^2 \times 2K^2)$ matrix, $\Omega_{\overline{b}}$ (or $\Omega_{\overline{h}}$) using **Eq. 2-33** (or **Eq. 2-35**)
2. Estimating the Cholesky factor of $\Omega_{\overline{b}}$ (or $\Omega_{\overline{h}}$)
3. Creating $\boldsymbol{D}_\pi$ (or $\boldsymbol{D}_\gamma$) using **Eq. 2-37** and estimating its eigenvalues
4. Finding the statistically significant threshold at specific α level, by knowing the asymptotic distribution of the estimator of $\left|\phi_{ij}(f)\right|^2$
5. If the null hypothesis is rejected, the variance and confidence interval of estimated connectivity measure should be calculated by finding the Ω_π (or Ω_γ), which is a scalar requiring multiplication of huge matrices discussed in **Table 2-2**, and their dimensions are provided in **Table 2-3**.
6. If there is not enough evidence to reject the null hypothesis, we can conclude that there is no significant connection between pair i,j at frequency.
7. Repeating steps 1-6 for all frequencies and all possible pairs.

Regarding the expensive computational cost of analytical verification of the estimated connectivity measures, as well as even more costly empirical procedure (shown in [21]), the modification of the algorithm is necessary to make it practicable for high-dimensional biological signals such as EEG. In the following chapter the development of the modified algorithm will be presented.

Table 2-2: The terms of the covariance of ϕ family, as explained in **Eq. 2-34**. *

$\nabla_{\overline{b}}\left\|\pi_{ij}(f)\right\|^2$	$2\left(\frac{\overline{b}^T I_{ij}^c (I_{2K}\otimes S_n) I_{ij}^c}{\overline{b}^T I_j^c (I_{2K}\otimes S_d) I_j^c \overline{b}} - \frac{\overline{b}^T I_{ij}^c (I_{2K}\otimes S_n) I_{ij}^c \overline{b}}{\left(\overline{b}^T I_j^c (I_{2K}\otimes S_d) I_j^c \overline{b}\right)^2} \overline{b}^T I_j^c (I_{2K}\otimes S_d) I_j^c\right)$
$\nabla_{\sigma}\left\|\pi_{ij}(f)\right\|^2$	$\frac{\left[\left(I_{ij}^c \overline{b}\right)^T \otimes \left(\overline{b}^T I_{ij}^c\right)\right]\Theta_K \varrho_n}{\overline{b}^T I_j^c (I_{2K}\otimes S_d) I_j^c \overline{b}} - \frac{\overline{b}^T I_{ij}^c (I_{2K}\otimes S_n) I_{ij}^c \overline{b}}{\left(\overline{b}^T I_j^c (I_{2K}\otimes S_d) I_j^c \overline{b}\right)^2}\left[\left(I_j^c \overline{b}\right)^T \otimes \left(\overline{b}^T I_j^c\right)\right]\Theta_K \varrho_d$
$\nabla_{\overline{h}}\left\|\gamma_{ij}(f)\right\|^2$	$2\left(\frac{\overline{h}^T I_{ij}^c (I_2\otimes S_n\otimes I_K) I_{ij}^c}{\overline{h}^T I_i^c (I_2\otimes S_d\otimes I_K) I_i^c \overline{h}} - \frac{\overline{h}^T I_{ij}^c (I_2\otimes S_n\otimes I_K) I_{ij}^c \overline{h}}{\left(\overline{h}^T I_i^c (I_2\otimes S_d\otimes I_K) I_i^c \overline{h}\right)^2} \overline{h}^T I_i^c (I_{2K}\otimes S_d) I_i^c\right)$
$\nabla_{\sigma}\left\|\gamma_{\mathrm{ij}}(f)\right\|^2$	$\frac{\left[\left(I_{ij}^c \overline{h}\right)^T \otimes \left(\overline{h}^T I_{ij}^c\right)\right]\Theta_K \varrho_n}{\overline{h}^T I_i^c (I_2\otimes S_d\otimes I_K) I_i^c \overline{h}} - \frac{\overline{h}^T I_{ij}^c (I_2\otimes S_n\otimes I_K) I_{ij}^c \overline{h}}{\left(\overline{h}^T I_i^c (I_2\otimes S_d\otimes I_K) I_i^c \overline{h}\right)^2}\left[\left(I_i^c \overline{h}\right)^T \otimes \left(\overline{h}^T I_i^c\right)\right]\Theta_K \varrho_d$
*I_{ij} is a matrix whose elements are zero except for the element corresponding to i,j whose value equals 1. I_j is a matrix made by zeros except K unit value elements located diagonally for the entries (l,m): $(j-1)K+1 \le l = m \le jK$. Also, I_j^c=$I_2 \otimes I_j$ and I_{ij}^c=$I_2 \otimes I_{ij}$.Θ_K is a function of commutation matrix, $T_{K,K}$, whose dimension is $K^2 \times K^2$. ϱ_n, ϱ_d and Θ_K for group π and group γ are introduced in [34]and [35].	

Table 2-3: Dimensions of the variables defined in **Table 2-2**

VARIABLES	$\overline{\boldsymbol{b}}$	$\boldsymbol{I_{ij}^{c}}$ $\boldsymbol{\mid I_{j}^{c}}$	$\boldsymbol{I_{2K}\otimes S_{n\mid d}}$	$\boldsymbol{\Theta_{K}}$	$\boldsymbol{\varrho_{n\mid d}}$
DIMENSIONS	$2K^2 \times 1$	$2K^2 \times 2K^2$	$2K^2 \times 2K^2$	$4K^4 \times \mathrm{K}^2$	$K^2 \times K^2$

CHAPTER 3

FAST ASYMPTOTIC ALGORITHM

The objective of this chapter is to provide the mathematical proofs involved in our optimization of the current state-of-the-art asymptotic algorithms for γ and π connectivity measures. It should be noted that the relationships developed in this chapter are simplified by skipping the dependency of variables on frequency.

3.1 Statistical Properties of the Variables

Since γ and π measures are continuous functions of H and B respectively and of Σ_e, the asymptotic distributions for each of these measures is first needed to be derived separately. The stepping stone in formulating the respective distributions is to define the statistical properties of the MVAR process and exploit the *delta method* theorem [31].

The asymptotic distribution of the estimators of $\boldsymbol{A}$, Σ_e, $\overline{h}$ and $\overline{b}$ are derived in [34, 35, 43] and were reviewed in chapter two (**Eq. 2-23**, **Eq. 2-24**, **Eq. 2-35**, and **Eq. 2-33**). To optimize the original asymptotic algorithm, we slightly changed the statistical properties of the input variables of the connectivity measures, including Σ_e, $\overline{h}$ and $\overline{b}$. These prerequisite modifications impressively influence the speed of the purposed algorithm.

3.1.1 Statistical Properties of $\boldsymbol{A}$

In our proposed algorithm the two terms of the $\Omega_{\boldsymbol{a}}$ in **Eq. 2-23**, $\Gamma_y^{-1}$and Σ_e**,** were initially decomposed so that $\Gamma_y^{-1} = L_\Gamma {L_\Gamma}^T$, and $\Sigma_e = L_e {L_e}^T$. As mentioned, $\Gamma_y^{-1}$and Σ_e are symmetric positive definite matrices, so the Cholesky factorization can be applied so that L_Γ and L_e are Cholesky factors of $\Gamma_y^{-1}$and Σ_e respectively. Then, **Eq. 2-23** can be written as:

$$\Omega_{\boldsymbol{a}} = L_\Gamma {L_\Gamma}^T \otimes L_e {L_e}^T = (L_\Gamma \otimes L_e)(L_\Gamma \otimes L_e)^T \qquad \textbf{Eq. 3-1}$$

Therefore, $L_{\boldsymbol{a}} = (L_\Gamma \otimes L_e)$ is the Cholesky factor of $\Omega_{\boldsymbol{a}}$.

3.1.2 Statistical Properties of $\overline{B}$

To find the asymptotic distribution of B, **Eq. 2-30** can be rewritten as:

$$\overline{B} = [I_K, 0_K] - \boldsymbol{A}(\mathcal{C}^T \otimes I_K) \qquad \textbf{Eq. 3-2}$$

where the $(K \times 2K)$ matrix $\overline{B}$ contains real and imaginary parts of B. If $\overline{b} \triangleq vec(\overline{B})$, the asymptotic distribution properties of the estimator of $\overline{b}$ were obtained by applying the *delta method*:

$$\sqrt{n_s}\left(\hat{\overline{b}} - \overline{b}\right) \xrightarrow{d} \mathcal{N}\left(0,\, \Omega_{\overline{b}}\right) \qquad \textbf{Eq. 3-3}$$

$$\Omega_{\overline{b}} = \left(\frac{\partial vec(\overline{B})}{\partial \boldsymbol{a}^T}\right) \Omega_a \left(\frac{\partial vec(\overline{B})}{\partial \boldsymbol{a}^T}\right)^T = (\mathcal{C} \otimes I_{k^2}) \Omega_{\boldsymbol{a}} (\mathcal{C}^T \otimes I_{k^2}) \qquad \textbf{Eq. 3-4}$$

Furthermore, the decomposition of **Eq. 3-4** in the form of $\Omega_{\overline{b}} \triangleq L_{\overline{b}} {L_{\overline{b}}}^T$ was done by substituting **Eq. 3-1** in **Eq. 3-4**:

$$L_{\overline{b}} = (\mathcal{C} \otimes I_{K^2})(L_\Gamma \otimes L_e) \qquad \textbf{Eq. 3-5}$$

3.1.3 Statistical Properties of $\overline{H}$

Similarly, to find the asymptotic distribution of $\overline{H}$ that is H in terms of real and imaginary parts obtained in [35], $\overline{H}$ was converted into matrix format. This format is very useful in reducing the time complexity of the algorithm as will be shown in the following sections. According to [35], for large values of n_s, $\overline{h} \triangleq vec(\overline{H})$ asymptotically converges to the normal distribution with the covariance $\Omega_{\overline{h}}$ shown in **Eq. 2-35**. We defined $\mathcal{H}$ as the summation of two conjugate terms:

$$\mathcal{H} = F_1 \otimes H^T \otimes H + F_2 \otimes H^H \otimes H^* \qquad \textbf{Eq. 3-6}$$

where $F_1 = \frac{1}{2}\begin{bmatrix} 1 & j \\ -j & 1 \end{bmatrix}$, $F_2 = \frac{1}{2}\begin{bmatrix} 1 & -j \\ j & 1 \end{bmatrix}$, and the superscript * represents the complex conjugate operator.

If we define $\Omega_{\overline{h}} \triangleq L_{\overline{h}} L_{\overline{h}}^T$, by substituting **Eq. 3-5** and **Eq. 3-6** in **Eq. 2-35**:

$$L_{\overline{h}} = (\{(F_1 \mathcal{C} \otimes H^T) L_\Gamma\} \otimes H L_e) + (\{(F_2 \mathcal{C} \otimes H^H) L_\Gamma\} \otimes H^* L_e) \qquad \textbf{Eq. 3-7}$$

$L_{\overline{h}}$ is frequency dependent. The following sections explain how **Eq. 3-7** and **Eq. 3-5** applied for optimization of the algorithm.

- **Proof of Eq. 3-6:**

According to [35]:

$$\mathcal{H} = (\rho \otimes I_{k^2}) \begin{bmatrix} (H^T \otimes H) & 0 \\ 0 & (H^T \otimes H)^* \end{bmatrix} (\rho^{-1} \otimes I_{k^2}) \qquad \textbf{Eq. 3-8}$$

where $\rho = \frac{1}{2}\begin{bmatrix} 1 & 1 \\ -j & j \end{bmatrix}$. Substituting ρ in **Eq. 3-8**, we further decompose the elements of $\mathcal{H}$ into sums of two conjugate terms:

$$\mathcal{H} = \frac{1}{2} \times \begin{bmatrix} (H^T \otimes H) + (H^T \otimes H)^* & \mathrm{j}(H^T \otimes H) - \mathrm{j}(H^T \otimes H)^* \\ -\mathrm{j}(H^T \otimes H) + \mathrm{j}(H^T \otimes H)^* & (H^T \otimes H) + (H^T \otimes H)^* \end{bmatrix} \qquad \textbf{Eq. 3-9}$$

Which is equivalent to:

$$\mathcal{H} = \frac{1}{2}\begin{bmatrix} 1 & \mathrm{j} \\ -\mathrm{j} & 1 \end{bmatrix} \otimes H^T \otimes H + \frac{1}{2}\begin{bmatrix} 1 & -\mathrm{j} \\ \mathrm{j} & 1 \end{bmatrix} \otimes H^H \otimes H^* \quad \textbf{Eq. 3-10}$$
$$= F_1 \otimes H^T \otimes H + F_2 \otimes H^H \otimes H^*$$

It is also worth to mention that $F_1F_2=0$, and $F_1F_1=F_1=F_1^H=F_2^T$. ■

3.1.4 Statistical Properties of Σ_e

Defining $\boldsymbol{\sigma} \triangleq vec(\Sigma_e)$, it is shown in [43] that the estimator of $\boldsymbol{\sigma}$ has an asymptotic normal distribution with the covariance, $\Omega_{\boldsymbol{\sigma}}=2D_K D_K^{+}(\Sigma_e \otimes \Sigma_e)D_K^{+T}D_K^T$, where D_K^{+} is the Moore-Penrose pseudo-inverse of the standard duplication matrix. In this study, by substituting $D_K D_K^{+}$ by ½ $\left(I_{K^2} + T_{K,K}\right)$, where $T_{K,K}$ is the commutation matrix with dimension of $(K^2 \times K^2)$, a more convenient form of $\Omega_{\boldsymbol{\sigma}}$ is introduced:

$$\Omega_{\boldsymbol{\sigma}} = (\Sigma_e \otimes \Sigma_e)\left(I_{K^2} + T_{K,K}\right) \quad \textbf{Eq. 3-11}$$

According to the definition of the commutation matrix (**Appendix A.2**), $T_{K,K}$ behaves like I_{K^2} when multiplied by the vec of a symmetric matrix [44]. This condition holds for $\Omega_{\boldsymbol{\sigma}}$ in all equations of this study and leads to simplification of **Eq. 3-11** to 2 $(\Sigma_e \otimes \Sigma_e)$.

3.2 Statistical Properties of Connectivity Measures

As it was mentioned in chapter two, the existence of a significant connectivity ϕ_{ij} at specific frequency f between two sites i and j is tested according to the following hypothesis:

$$H_0 : \left|\phi_{ij}\right|^2 = 0 \qquad \forall\, i,j \in \{1,\dots,K\} \quad \textbf{Eq. 3-12}$$

Rejecting the H_0 at α statistical significance level provides a strong conclusion for the existence of a significant connectivity. The confidence intervals for the statistically

significant connections are then estimated by determining the asymptotic distribution of the estimator of $|\phi_{ij}|^2$ measures.

3.2.1 Asymptotic Distribution in Non-Null Case

To approximate the distribution of the real differentiable function $|\phi_{ij}|^2$, the *delta method* was implemented. According to [34] and [35], the distribution of $\sqrt{n_s}\left(|\hat{\phi}_{ij}|^2 - |\phi_{ij}|^2\right)$ asymptotically converges to normal distribution with zero mean and covariance Ω_ϕ for large n_s . It was shown in **Eq. 2-34** that since $|\phi_{ij}|^2$ is a function of $\boldsymbol{\sigma}$ and either $\overline{b}$ or $\overline{h}$, Ω_ϕ can be estimated as the summation of the covariance $|\phi_{ij}|^2$with respect to its variables.

Decomposing the ϕ connectivity measures as in **Eq. 2-11**, the fraction derivative formula can be applied to estimate the terms in the right-hand side of **Eq. 2-34** as:

$$\nabla_\psi \phi^2 = \frac{\partial |\phi_{ij}|^2}{\partial \psi^T} = \frac{1}{\phi_d}\left(\frac{\partial \phi_n}{\partial \psi^T} + |\phi_{ij}|^2 \frac{\partial \phi_d}{\partial \psi^T}\right) \qquad \textbf{Eq. 3-13}$$

where ψ can be either $\boldsymbol{\sigma}$ or $\overline{h}(f)$ or $\overline{b}(f)$ in group γ and group π, respectively.

By implementing the properties of vec operation provided in **Appendix A.1**, separating the equations in terms of the variables i , j , and f, and using **Eq. 3-2**, **Eq. 3-6** and **Eq. 3-11**, we decreased the dimension of the covariance matrices in **Eq. 2-34** and therefore the complexity of the algorithm.

Statistical properties of group γ

By defining $|\gamma_{ij}|^2 \triangleq \gamma_n/\gamma_d$, as $\Omega_\gamma = \Omega_{\gamma_{\overline{h}}} + \Omega_{\gamma_{\boldsymbol{\sigma}}}$, $\Omega_{\gamma_{\overline{h}}}$ and $\Omega_{\gamma_{\boldsymbol{\sigma}}}$was obtained by applying the *delta method* and **Eq. 3-13**.

1. Estimation of $\Omega_{\gamma_{\overline{h}}}$: $|\gamma_{ij}|^2$ is defined as:

$$\left|\gamma_{ij}\right|^2 = \frac{\gamma_n}{\gamma_d} = \frac{\overline{h}^T T_n \overline{h}}{\overline{h}^T T_d \overline{h}} \qquad \textbf{Eq. 3-14}$$

where T_n and T_d are defined in Table 3-1 and Table 3-2. $\nabla_{\overline{h}}\gamma^2$ can be estimated when ϕ and ψ are replaced by γ and $\overline{h}$ in **Eq. 3-13**, respectively. According to (**Eq. A-4**), $\partial\gamma_n/\partial\overline{h}^T = 2\,\overline{h}^T T_n$, and $\partial\gamma_d/\partial\overline{h}^T = 2\,\overline{h}^T T_d$, then:

$$\nabla_{\overline{h}}\gamma^2 = \frac{2}{\gamma_d}\left(\overline{h}^T T_n - \left|\gamma_{ij}\right|^2 \overline{h}^T T_d\right) \qquad \textbf{Eq. 3-15}$$

According to **Table 3-1**, **Table 3-2** and using the vec properties in (**Appendix A.1**):

$$\overline{h}^T T_n = vec(\overline{H})^T\{I_2 \otimes E_j\, S_n \otimes E_i\} = vec\left\{E_i\, \overline{H}\,(I_2 \otimes E_j S_n)\right\}^T \qquad \textbf{Eq. 3-16}$$

where E_j is a matrix with dimension $K \times K$ whose j^{th}entries in the main diagonal are 1 and the rest of the entries are zero. Applying the same properties for the denominator:

$$\overline{h}^T T_d = vec(\overline{H})^T\{I_2 \otimes S_d \otimes E_i\} = vec\left\{E_i\, \overline{H}\,(I_2 \otimes S_d)\right\}^T \qquad \textbf{Eq. 3-17}$$

Substituting **Eq. 3-16** and **Eq. 3-17** in **Eq. 3-15** :

$$\nabla_{\overline{h}}\gamma^2 = \frac{2}{\gamma_d} vec\left(E_i\, \overline{H}\left\{I_2 \otimes \left(E_j S_n - |\gamma_{ij}|^2 S_d\right)\right\}\right)^T \qquad \textbf{Eq. 3-18}$$

So, $\nabla_{\overline{h}}\gamma^2$ can be written as $2/\gamma_d\; vec\left(W_{\overline{H}}\right)^T$. $\Omega_{\gamma_{\overline{h}}}$ can be estimated using **Eq. 3-18** and **Eq. 2-34**. By introducing $q \triangleq vec\left(W_{\overline{H}}\right)^T \mathcal{H}(\mathcal{C} \otimes I_{k^2})$, assuming $q = vec(Q)$, and applying (**Eq. A-7**), $\Omega_{\gamma_{\overline{h}}}$ is:

$$\Omega_{\gamma_{\overline{h}}} = \frac{4}{{\gamma_d}^2} trace\left(\Sigma_e Q \Gamma_y^{-1} Q^T\right) \qquad \textbf{Eq. 3-19}$$

where Q can be estimated as:

$$q = vec\left(W_{\overline{H}}\right)^T (F_1 \mathcal{C} \otimes H^T \otimes H + F_2 \mathcal{C} \otimes H^H \otimes H^*)$$
$$= vec\left\{H^T W_{\overline{H}} (F_1 \mathcal{C} \otimes H^T) + H^H W_{\overline{H}} (F_2 \mathcal{C} \otimes H^H)\right\}^T \quad \textbf{Eq. 3-20}$$

Substituting **Eq. 3-20** in **Eq. 3-19**:

$$\Omega_{\gamma_{\overline{h}}} = \frac{8}{{\gamma_d}^2} Real\{trace\left(\Sigma_e H^T W_{\overline{H}} (F_1 C \otimes H^T) \Gamma_y^{-1} (C^T F_2 \otimes H) {W_{\overline{H}}}^T H\right)$$
$$+ trace\left(\Sigma_e H^T W_{\overline{H}} (F_1 C \otimes H^T) \Gamma_y^{-1} (C^T F_1 \otimes H^*) {W_{\overline{H}}}^T H^*\right)\} \quad \textbf{Eq. 3-21}$$

By replacing $W_{\overline{H}}$ in **Eq. 3-21**, $\Omega_{\gamma_{\overline{h}}}$ is converted into the summation of eight terms which can be summarized as:

$$\Omega_{\gamma_{\overline{h}}} = \frac{8}{{\gamma_d}^2} \left({S_{n,jj}}^2 T_1(i,j) + \left|\gamma_{ij}\right|^4 T_2(i) - 2 S_{n,jj} \left|\gamma_{ij}\right|^2 T_3(i,j)\right) \quad \textbf{Eq. 3-22}$$

where $S_{n,jj}$ is the j^{th} element of the main diagonal of S_n:

$$T_1(i,j) = Real\left\{\mu_{\gamma 1,i} \left(\overline{H}_{ij} {g_{p\gamma}}^T {g_{p\gamma}}^T {\overline{H}^T}_{ij}\right)\right.$$
$$\left. + \mu_{\gamma 2,i} \left(\overline{H}_{ij} g_{p\gamma} {g_{p\gamma}}^H {\overline{H}^T}_{ij}\right)\right\} \quad \textbf{Eq. 3-23}$$

$$T_2(i) = Real\left\{\mu_{\gamma 1,i} e_i^T \overline{H} (F_1 C \otimes S_d H^T) \Gamma_y^{-1} (C^T F_2 \otimes H S_d) \overline{H}^T e_i\right.$$
$$\left. + \mu_{\gamma 2,i} e_i^T \overline{H} (F_1 C \otimes S_d H^T) \Gamma_y^{-1} (C^T F_1 \otimes H^* S_d) \overline{H}^T e_i\right\} \quad \textbf{Eq. 3-24}$$

$$T_3(i,j) = Real\left\{\mu_{\gamma 1,i} \overline{H}_{ij} g_{p\gamma} {L_\Gamma}^T (C^T F_2 \otimes H S_d) \overline{H}^T e_i\right.$$
$$\left. + \mu_{\gamma 2,i} \overline{H}_{ij} g_{p\gamma} {L_\Gamma}^T (C^T F_1 \otimes H^* S_d) \overline{H}^T e_i\right\} \quad \textbf{Eq. 3-25}$$

where $\mu_{\gamma 1,i}$ and $\mu_{\gamma 2,i}$ are the i^{th} element of the main diagonal of $H\Sigma_e H^T$ and $H\Sigma_e H^H$, respectively, $\overline{H}_{ij}$ is a (1×2) matrix containing the real and imaginary part of H_{ij}, e_i is a K-dimensional vector with i^{th} element equals one while remaining elements are zero,

and $g_{p\gamma} = F_1 C\left(I_p \otimes e_j^T H^T\right) L_\Gamma$. Considering **Eq. 3-22** to **Eq. 3-25** and **Appendix B.1,** the complexity for computing T_1 , T_2, T_3, and subsequently $\Omega_{\gamma_{\bar{h}}}$ is $O(K^3 p^2)$.

2. Estimation of Ω_{γ_σ}: Ω_{γ_σ} was estimated by finding the derivative of the group γ functions provided in **Table 2-1**. Since these equations implicitly separated the variable $\boldsymbol{\sigma}$, their partial derivatives have a convenient format.

Applying **Eq. 3-13** leads to $\nabla_\sigma \gamma^2 = 0$ for DTF. In the cases of $gDTF$ and $iDTF$, σ_{mm} was replaced by ${e_m}^T S_n e_m$ in the numerator. Using chain rule:

$$\frac{\partial \gamma_n}{\partial \boldsymbol{\sigma}^T} = \left(|H_{ij}|\right)^2 \frac{\partial {e_j}^T S_n e_j}{\partial \boldsymbol{\sigma}^T} = \left(|H_{ij}|\right)^2 \left({e_j}^T \otimes {e_j}^T\right) \frac{\partial vec(S_n)}{\partial \boldsymbol{\sigma}^T} \qquad \textbf{Eq. 3-26}$$

According to **Eq. A-6**, for $gDTF$ and $iDTF$, $\partial vec(S_n)/\partial \boldsymbol{\sigma}^T = diag(vec(I_K))$, where $diag(x)$ is a diagonal matrix whose main diagonal entries are vector x. Furthermore, ${e_j}^T \otimes {e_j}^T$ is the equivalent of $vec(E_j)^T$. Hence, for $gDTF$ and $iDTF$ we can write:

$$\begin{aligned} \frac{\partial \gamma_n}{\partial \boldsymbol{\sigma}^T} &= |H_{ij}|^2 vec\left(E_j\right)^T diag\left(vec(I_K)\right) = |H_{ij}|^2 vec\left(E_j \odot I_K\right)^T \\ &= vec\left(|H_{ij}|^2 E_j\right)^T \end{aligned} \qquad \textbf{Eq. 3-27}$$

where $\odot$ is the Hadamard operator or element-wise product. The derivative of the denominator which is a function of i, was obtained by finding the summation of the derivatives of the numerator over all values of j. Hence, for $gDTF$:

$$\begin{aligned} \frac{\partial \gamma_d}{\partial \boldsymbol{\sigma}^T} &= \sum_{m=1}^{K} \frac{\partial \gamma_n}{\partial \boldsymbol{\sigma}^T} \Big|_{j=m} = \sum_{m=1}^{K} vec(|H_{im}|^2 E_m)^T \\ &= vec\{diag(|{e_i}^T H|^2)\}^T \end{aligned} \qquad \textbf{Eq. 3-28}$$

If we substitute the denominator of $iDTF$ introduced in **Table 2-1** with $\sum_{m=1}^{K}(Real(H_{im} {e_i}^T H) S_d e_m)$, the derivative formula for $iDTF$ can be written as:

$$\frac{\partial \gamma_d}{\partial \boldsymbol{\sigma}^T} = \sum_{m=1}^{K} Real(H_{im} {e_i}^T H) \frac{\partial S_d e_m}{\partial \boldsymbol{\sigma}^T}$$
$$= Real\left(\sum_{m=1}^{K} (H_{im} {e_i}^T H)(e_m^T \otimes I_k) \frac{\partial S_d}{\partial \boldsymbol{\sigma}^T} \right) \quad \textbf{Eq. 3-29}$$

where $\partial vec(S_d)/\partial \boldsymbol{\sigma}^T = I_{k^2}$. According to the vectorization properties in **Appendix A.1**:

$$\frac{\partial \gamma_d}{\partial \boldsymbol{\sigma}^T} = Real\left(vec \sum_{m=1}^{K} (H_{im} e_m {e_i}^T H)^T \right) \quad \textbf{Eq. 3-30}$$

where:

$$\sum_{m=1}^{K} (H_{im} e_m {e_i}^T H) = \left(\sum_{m=1}^{K} (H_{im} e_m) \right) {e_i}^T H = H^H e_i {e_i}^T H \quad \textbf{Eq. 3-31}$$

By plugging **Eq. 3-31** into **Eq. 3-30**:

$$\frac{\partial \gamma_d}{\partial \boldsymbol{\sigma}^T} = Real\ (vec(H^H E_i H)^T) \quad \textbf{Eq. 3-32}$$

Finally, we can find $\nabla_{\boldsymbol{\sigma}} \gamma$, for *gDTF* by replacing **Eq. 3-27** and **Eq. 3-28** into **Eq. 3-13**:

$$\nabla_{\boldsymbol{\sigma}} \gamma^2 = \frac{1}{\gamma_d} vec\left\{ \left| H_{ij} \right|^2 E_j - |\gamma_{ij}|^2 diag(|{e_i}^T H|^2) \right\}^T \quad \textbf{Eq. 3-33}$$

And, for $iDTF$, by replacing **Eq. 3-27** and **Eq. 3-32** into **Eq. 3-13**:

$$\nabla_{\boldsymbol{\sigma}} \gamma^2 = \frac{1}{\gamma_d} vec\left\{ \left| H_{ij} \right|^2 E_j - |\gamma_{ij}|^2 Real(H^H E_i H) \right\}^T \quad \textbf{Eq. 3-34}$$

Therefore, $\nabla_{\boldsymbol{\sigma}} \gamma^2$ can be summarized in the format of $1/\gamma_d\ vec(W_{\boldsymbol{\sigma}})^T$. Substituting **Eq. 3-11**, and applying the properties of vec operator, $\Omega_{\gamma_{\boldsymbol{\sigma}}}$ can be rewritten as:

$$\Omega_{\gamma_{\boldsymbol{\sigma}}} = \frac{1}{{\gamma_d}^2}\ vec(\Sigma_e W_{\boldsymbol{\sigma}} \Sigma_e)\left(I_{K^2} + T_{K,K}\right) vec(W_{\boldsymbol{\sigma}}) \quad \textbf{Eq. 3-35}$$

Since $\Sigma_e W_\sigma \Sigma_e$ is symmetric, $vec(\Sigma_e W_{\boldsymbol{\sigma}} \Sigma_e) T_{K,K} = vec(\Sigma_e W_{\boldsymbol{\sigma}} \Sigma_e)$. Rewriting **Eq. 3-35**:

$$\Omega_{\gamma_{\boldsymbol{\sigma}}} = \frac{2}{{\gamma_d}^2} vec(\Sigma_e W_{\boldsymbol{\sigma}} \Sigma_e) vec(W_{\boldsymbol{\sigma}}) = \frac{2}{{\gamma_d}^2}\ trace(\Sigma_e W_{\boldsymbol{\sigma}} \Sigma_e W_{\boldsymbol{\sigma}}) \qquad \textbf{Eq. 3-36}$$

By replacing $W_{\boldsymbol{\sigma}}$ in **Eq. 3-36**, $\Omega_{\gamma_{\boldsymbol{\sigma}}}$ can be summarized as:

$$\Omega_{\gamma_{\boldsymbol{\sigma}}} = \frac{2}{\gamma_d^2}\left(|H_{ij}|^4 T_1(j) + \left|\gamma_{ij}\right|^4 T_2(i) - 2|H_{ij}|^2 \left|\gamma_{ij}\right|^2 T_3(i,j)\right) \qquad \textbf{Eq. 3-37}$$

where T_1, T_2, and T_3 are provided in **Table 3-4**. According to **Table 3-4** and **Appendix B.1**, T_1, T_2, T_3, and subsequently $\Omega_{\gamma_{\boldsymbol{\sigma}}}$ can be solved in $O(K^3)$ operations.

- **Proof of Eq. 3-37 and parameters in Table 3-4:**

By replacing $W_{\boldsymbol{\sigma}}$ in **Eq. 3-36**, for $gDTF$:

$$\begin{aligned}\Omega_{\gamma\boldsymbol{\sigma}} = \frac{2}{\gamma_d^2}\Big(&|H_{ij}|^4 trace\left(\Sigma_e E_j \Sigma_e E_j\right) \\ &+ \left|\gamma_{ij}\right|^4 trace\left(\Sigma_e diag(|e_i^T H|^2)\Sigma_e diag(|e_i^T H|^2)\right) \\ &- 2|H_{ij}|^2\left|\gamma_{ij}\right|^2 trace\left(\Sigma_e E_j \Sigma_e diag(|e_i^T H|^2)\right)\Big)\end{aligned} \qquad \textbf{Eq. 3-38}$$

Then:

$$T_1(j) = trace\left(\Sigma_e E_j \Sigma_e E_j\right) = {e_j}^T(\Sigma_e \odot \Sigma_e) e_j = \boldsymbol{\sigma}_{jj}^2 \qquad \textbf{Eq. 3-39}$$

$$\begin{aligned}T_2(i) &= trace\left(\Sigma_e diag(|e_i^T H|^2)\Sigma_e diag(|e_i^T H|^2)\right) \\ &= e_i^T (H \odot H^*)^T (\Sigma_e \odot \Sigma_e)(H \odot H^*) e_i\end{aligned} \qquad \textbf{Eq. 3-40}$$

$$T_3(i,j) = trace\left(\Sigma_e E_j \Sigma_e diag(|e_i^T H|^2)\right) = e_i^T (H \odot H^*)^T (\Sigma_e \odot \Sigma_e) e_j \qquad \textbf{Eq. 3-41}$$

For $iDTF$, substituting $Real(H^H E_i H)$ with $(H^H E_i H + H^T E_i H^*)/2$, results in:

$$\Omega_{\gamma\sigma} = \frac{2}{\gamma_d^2}\Bigg\{|H_{ij}|^4 trace\left(\Sigma_e E_j \Sigma_e E_j\right)$$

$$+ \frac{\left|\gamma_{ij}\right|^4}{4} trace(\Sigma_e H^H E_i H \Sigma_e H^H E_i H$$

$$+ \Sigma_e H^T E_i H^* \Sigma_e H^T E_i H^* + 2\Sigma_e H^H E_i H \Sigma_e H^T E_i H^*)$$

$$- |H_{ij}|^2 \left|\gamma_{ij}\right|^2 trace\left(\Sigma_e E_j \Sigma_e H^H E_i H + \Sigma_e E_j \Sigma_e H^T E_i H^*\right)\Bigg\} \qquad \textbf{Eq. 3-42}$$

$T_1(i)$ is the same as that of $gDTF$. The first two terms of $T_2(j)$ are equivalent:

$$T_2(i) = \frac{1}{2} trace(\Sigma_e H^H E_i H \Sigma_e H^H E_i H + \Sigma_e H^H E_i H \Sigma_e H^T E_i H^*)$$

$$= \frac{1}{2}(e_i{}^T (H\Sigma_e H^H) e_i \; e_i{}^T (H\Sigma_e H^H) e_i$$

$$+ e_i{}^T (H\Sigma_e H^T)^H e_i \; e_i{}^T (H\Sigma_e H^T) e_i) = \qquad \textbf{Eq. 3-43}$$

$$= \frac{1}{2}\left(\left|\mu_{\gamma 1,i}\right|^2 + \left|\mu_{\gamma 2,i}\right|^2 \right)$$

$T_3(i,j)$ is the summation of two equal terms, so:

$$T_3(i,j) = trace\left(H\Sigma_e E_j \Sigma_e H^H E_i\right) = e_i{}^T (H\Sigma_e \odot H^* \Sigma_e) e_j \qquad \textbf{Eq. 3-44}$$

Table 3-1: Variables T_n and T_d for groups of connectivity

VARIABLES	GROUP γ	GROUP π
$\boldsymbol{T_n(i,j,\sigma)}$	$I_2 \otimes E_j S_n \otimes E_i$	$I_2 \otimes E_j \otimes E_i S_n$
$\boldsymbol{T_d(i,j,\sigma)}$	$I_2 \otimes S_d \otimes E_i$	$I_2 \otimes E_j \otimes S_d$

Table 3-2: Variables S_n and S_d for connectivity measures

	$\boldsymbol{DTF}$	$\boldsymbol{gDTF}$	$\boldsymbol{iDTF}$	$\boldsymbol{PDC}$	$\boldsymbol{gPDC}$	$\boldsymbol{iPDC}$
$\boldsymbol{S_n}$	I_k	$(\Sigma_e \odot I_k)$	$(\Sigma_e \odot I_k)$	I_k	$(\Sigma_e \odot I_k)^{-1}$	$(\Sigma_e \odot I_k)^{-1}$
$\boldsymbol{S_d}$	I_k	$(\Sigma_e \odot I_k)$	Σ_e	I_k	$(\Sigma_e \odot I_k)^{-1}$	${\Sigma_e}^{-1}$

Statistical properties of group π

By defining $|\pi_{ij}|^2 \triangleq \pi_n/\pi_d$, as $\Omega_\pi = \Omega_{\pi_{\overline{b}}} + \Omega_{\pi_{\boldsymbol{\sigma}}}$, $\Omega_{\pi_{\overline{b}}}$ and $\Omega_{\pi_{\boldsymbol{\sigma}}}$was obtained by applying the *delta method*.

1. Estimation of $\Omega_{\pi_{\overline{b}}}$: Similar to $\Omega_{\pi_{\overline{h}}}$, for group π, we can write:

$$|\pi_{ij}|^2 = \frac{\pi_n}{\pi_d} = \frac{\overline{b}^T T_n \overline{b}}{\overline{b}^T T_d \overline{b}} \qquad \textbf{Eq. 3-45}$$

where T_n and T_d are defined in **Table 3-1** and **Table 3-2**. Substituting $\partial\pi_n/\partial\overline{b}^T = 2\,\overline{b}^T T_n$, and $\partial\pi_d/\partial\overline{b}^T = 2\,\overline{b}^T T_d$ into **Eq. 3-13**, where ϕ and ψ are replaced by π and $\overline{b}$:

$$\nabla_{\overline{b}}\pi^2 = \frac{2}{\pi_d}\left(\overline{b}^T T_n - |\pi_{ij}|^2\,\overline{b}^T T_d\right) \qquad \textbf{Eq. 3-46}$$

According to **Table 3-1** and **Table 3-2** and using the vec properties:

$$\overline{b}^T T_n = vec(\overline{B})^T\{I_2 \otimes E_j \otimes E_i S_n\} = vec\{S_n E_i\,\overline{B}\,(I_2 \otimes E_j)\}^T \qquad \textbf{Eq. 3-47}$$

$$\overline{b}^T T_d = vec(\overline{B})^T\{I_2 \otimes E_j \otimes S_d\} = vec\{{S_d}^T\,\overline{B}\,(I_2 \otimes E_j)\}^T \qquad \textbf{Eq. 3-48}$$

Substituting **Eq. 3-47** and **Eq. 3-48** in **Eq. 3-46**:

$$\nabla_{\overline{b}}\pi^2 = \frac{2}{\pi_d}\,vec\{(S_n E_i - |\pi_{ij}|^2 {S_d}^T)\overline{B}\,(I_2 \otimes E_j)\}^T \qquad \textbf{Eq. 3-49}$$

$\nabla_{\overline{b}}\pi^2$ can be replaced by $2/\pi_d\,vec(W_{\overline{b}})^T$. According to the *delta method*, $\Omega_{\pi_{\overline{b}}}$ equals $(\nabla_{\overline{b}}\pi^2)\Omega_{\overline{b}}(\nabla_{\overline{b}}\pi^2)^T$. Replacing **Eq. 3-4**, and using the vec properties results:

$$\Omega_{\pi_{\bar{b}}} = \frac{4}{{\pi_d}^2} vec\{W_{\bar{b}}(\mathcal{C}\otimes I_K)\}^T \Omega_{\boldsymbol{a}}\, vec\{W_{\bar{b}}(\mathcal{C}\otimes I_K)\} \qquad \textbf{Eq. 3-50}$$

Substituting $I_2\otimes E_j$ by $(I_2\otimes e_j)(I_2\otimes {e_j}^T)$ in **Eq. 3-49**, since $(I_2\otimes {e_j}^T)(\mathcal{C}\otimes I_K) = \mathcal{C}(I_P\otimes {e_j}^T)$), Q can be defined as:

$$Q = \left[(S_n E_i - |\pi_{ij}|^2 {S_d}^T)\overline{B}\,(I_2\otimes e_j)\right]_{K\times 2} \qquad \textbf{Eq. 3-51}$$

The $(K \times 2)$ matrix Q is the multiplier of the real and imaginary values of B in column j^{th}. $\Omega_{\pi_{\bar{b}}}$ can be written as:

$$\Omega_{\pi_{\bar{b}}} = \frac{4}{{\pi_d}^2} trace\left(\Sigma_e Q G_p Q^T\right) \qquad \textbf{Eq. 3-52}$$

where $G_p(j,f) = [\mathcal{C}]_{2\times p}\left[(I_P\otimes {e_j}^T)\,\Gamma_y^{-1}(I_P\otimes e_j)\right]_{P\times P}[\mathcal{C}^T]_{p\times 2}$ is a (2×2) matrix whose middle term is a subset of Γ_y^{-1}. Substituting **Eq. 3-51** in **Eq. 3-52**:

$$\Omega_{\pi\bar{b}} = \frac{4}{\pi_d^2} trace\Bigg(\Big(S_n E_i - |\pi_{ij}|^2 S_d\Big)\Sigma_e\Big(S_n E_i - |\pi_{ij}|^2 S_d\Big)\overline{B}(I_2\otimes e_j)G_p(I_2\otimes e_j^T)\overline{B}^T\Bigg) \qquad \textbf{Eq. 3-53}$$

Finally, **Eq. 3-53** can be summarized as:

$$\Omega_{\pi\bar{b}} = \frac{4}{\pi_d^2}\Big(S_{n,ii}{}^2 T_1(i,j) + |\pi_{ij}|^4 T_2(j) - 2S_{n,ii}|\pi_{ij}|^2 T_3(i,j)\Big) \qquad \textbf{Eq. 3-54}$$

where T_1, T_2, and T_3 can be found in **Table 3-3**. In **Table 3-3**, J_K is K-dimensional vector with entries of one, $\overline{B}_{ij}$ is a (1×2) matrix containing the real and imaginary part of B_{ij}, $\overline{B}(I_2\otimes e_j)G_p(I_2\otimes e_j^T)\overline{B}^T$ is a $(K \times K)$ matrix obtained by multiplying three matrices of dimensions $(K \times 2)$, (2×2), and $(2 \times K)$. According to **Table 3-3** and **Appendix B.1**, computation of T_1 , T_2, T_3, and subsequently $\Omega_{\pi_{\bar{b}}}$ involves $O(K^3 + Kp^2)$ operations.

Table 3-3: Defining variables T_1, T_2, and T_3 in **Eq. 3-54**

	PDC	***gPDC***	***iPDC***
$\boldsymbol{T_1}$	$\sigma_{ii}\overline{B}_{ij}G_p\overline{B}^T{}_{ij}$		
$\boldsymbol{T_2}$	${J_K}^T\begin{pmatrix}\Sigma_e\odot\overline{B}\left(I_2\otimes e_j\right)\\ G_p\left(I_2\otimes e_j^T\right)\overline{B}^T\end{pmatrix}J_K$	${J_K}^T S_n\begin{pmatrix}\Sigma_e\odot\overline{B}\left(I_2\otimes e_j\right)\\ G_p\left(I_2\otimes e_j^T\right)\overline{B}^T\end{pmatrix}S_nJ_K$	${J_K}^T\begin{pmatrix}{\Sigma_e}^{-1}\odot\overline{B}\left(I_2\otimes e_j\right)\\ G_p\left(I_2\otimes e_j^T\right)\overline{B}^T\end{pmatrix}J_K$
$\boldsymbol{T_3}$	${e_i}^T\begin{pmatrix}\Sigma_e\odot\overline{B}\left(I_2\otimes e_j\right)\\ G_p\left(I_2\otimes e_j^T\right)\overline{B}^T\end{pmatrix}J_K$	${e_i}^T\begin{pmatrix}\Sigma_e\odot\overline{B}\left(I_2\otimes e_j\right)\\ G_p\left(I_2\otimes e_j^T\right)\overline{B}^T\end{pmatrix}S_nJ_K$	$\overline{B}_{ij}G_p\overline{B}^T{}_{ij}$

2. Estimation of $\Omega_{\pi_{\boldsymbol{\sigma}}}$: Deriving $\Omega_{\pi_{\boldsymbol{\sigma}}}$ follows the same steps used for $\Omega_{\gamma_{\boldsymbol{\sigma}}}$.

While for $DC\ \nabla_{\boldsymbol{\sigma}}\pi = 0$, for $gPDC$ and $iPDC$ we can write:

$$\frac{\partial\pi_n}{\partial\boldsymbol{\sigma}^T} = |B_{ij}|^2\frac{\partial(e_i{}^T S_n e_i)}{\partial\boldsymbol{\sigma}^T} = |B_{ij}|^2({e_i}^T\otimes {e_i}^T)\frac{\partial vec(S_n)}{\partial\boldsymbol{\sigma}^T} \qquad \textbf{Eq. 3-55}$$

According to **Eq. A-5** and **Eq. A-6**, $\partial vec(S_n)/\partial\boldsymbol{\sigma}^T = (-S_n^T\otimes S_n)diag\left(vec(I_K)\right)$, and S_n is diagonal. So, **Eq. 3-55** is simplified as:

$$\begin{aligned}\frac{\partial\pi_n}{\partial\boldsymbol{\sigma}^T} &= \left|B_{ij}\right|^2 vec(-S_nE_iS_n)^T diag\left(vec(I_K)\right)\\ &= \left|B_{ij}\right|^2 vec(-S_nE_iS_n\odot I_K)^T = vec\left(-\left|B_{ij}\right|^2 E_i{S_n}^2\right)^T\end{aligned} \qquad \textbf{Eq. 3-56}$$

For $gPDC$, $\partial\pi_d/\partial\boldsymbol{\sigma}^T$ can be written as the summation of derivatives:

$$\begin{aligned}\frac{\partial\pi_d}{\partial\boldsymbol{\sigma}^T} &= \sum_{m=1}^{K}\frac{\partial\pi_n}{\partial\boldsymbol{\sigma}^T}\,|_{i=m} = \sum_{m=1}^{K} vec\left(\left|B_{mj}\right|^2 E_m{S_n}^2\right)^T\\ &= vec\left\{-diag\left(\left|Be_j\right|^2\right){S_n}^2\right\}^T\end{aligned} \qquad \textbf{Eq. 3-57}$$

By substituting the denominator of $iPDC$ defined in **Table 2-1** with $\sum_{m=1}^{K} Real(B_{mj}{e_j}^T B^H)S_d\ e_m$:

$$\frac{\partial \pi_d}{\partial \boldsymbol{\sigma}^T} = \sum_{m=1}^{K} Real(B_{mj} {e_j}^T B^H) \frac{\partial S_d e_m}{\partial \boldsymbol{\sigma}^T}$$

$$= Real\left(\sum_{m=1}^{K} \left(B_{mj} {e_j}^T B^H\right)(e_m^T \otimes I_k) \frac{\partial S_d}{\partial \boldsymbol{\sigma}^T} \right) \quad \textbf{Eq. 3-58}$$

where $\partial vec(S_d)/\partial \boldsymbol{\sigma}^T = (-S_d^T \otimes S_d)$.

Applying vec properties **(Appendix A.1)**:

$$\frac{\partial \pi_d}{\partial \boldsymbol{\sigma}^T} = Real\left\{ \sum_{m=1}^{K} vec\left(e_m B_{mj} {e_j}^T B^H\right)^T \ (-S_d^T \otimes S_d) \right\}$$

$$= Real\left\{ vec\left(\left\{ \sum_{m=1}^{K} \left(e_m B_{mj}\right) \right\} {e_j}^T B^H \right)^T (-S_d^T \otimes S_d) \right\} \quad \textbf{Eq. 3-59}$$

$$= Real\left\{ vec\left(B e_j {e_j}^T B^H\right)^T \right\} (-S_d^T \otimes S_d)$$

$$= Real\left\{ vec\left(B E_j B^H\right)^T (-S_d^T \otimes S_d) \right\}$$

$$\frac{\partial \pi_d}{\partial \boldsymbol{\sigma}^T} = -Real\left(vec\left(S_d^T B E_j B^H S_d^T\right)^T \right) \quad \textbf{Eq. 3-60}$$

Finally, $\nabla_{\boldsymbol{\sigma}} \pi^2$ can be obtained by substituting ϕ and ψ with π and $\boldsymbol{\sigma}$ in **Eq. 3-13** respectively. For $gPDC$:

$$\nabla_{\boldsymbol{\sigma}} \pi^2 = \frac{1}{\pi_d} vec\left\{ -\left|B_{ij}\right|^2 E_i {S_n}^2 + |\pi_{ij}|^2 diag\left(\left|B\ e_j\right|^2\right) {S_n}^2 \right\}^T \quad \textbf{Eq. 3-61}$$

For $iPDC$:

$$\nabla_{\boldsymbol{\sigma}} \pi^2 = \frac{1}{\pi_d} vec\left\{ -\left|B_{ij}\right|^2 E_i {S_n}^2 + |\pi_{ij}|^2 Real\left(S_d^T B E_j B^H S_d^T\right) \right\}^T \quad \textbf{Eq. 3-62}$$

Therefore, $\nabla_{\boldsymbol{\sigma}} \pi^2$ can be summarized in the format of $1/\pi_d \ vec(W_{\boldsymbol{\sigma}})^T$, and $\Omega_{\pi_{\boldsymbol{\sigma}}}$ has the same relation as that obtained for group γ in **Eq. 3-36**. Finally, $\Omega_{\pi_{\boldsymbol{\sigma}}}$ can be rewritten as:

$$\Omega_{\pi_\sigma} = \frac{2}{\pi_d^2}\left(|B_{ij}|^4 T_1(i) + \left|\pi_{ij}\right|^4 T_2(j) - |B_{ij}|^2\left|\pi_{ij}\right|^2 T_3(i,j)\right) \qquad \textbf{Eq. 3-63}$$

where T_1, T_2, and T_3 are provided in **Table 3-4**. We skipped the proof of **Eq. 3-63** since it is similar to the proof of **Eq. 3-37** which was explained in the previous section. In **Table 3-4**, $\mu_{\pi 1,j}$ and $\mu_{\pi 2,j}$ are the j^{th} element of the main diagonal of $B^T{\Sigma_e}^{-1}B$ (the inverse of $H\Sigma_e H^T$) and $B^H{\Sigma_e}^{-1}B$ (the inverse of $H\Sigma_e H^H$), respectively. According to **Table 3-4** and **Appendix B.1**, calculation of T_1 , T_2, T_3, and subsequently Ω_{π_σ}requires $O(K^3)$ operations.

Table 3-4: Defining variables T_1, T_2, and T_3 for estimating Ω_{ϕ_σ} in **Eq. 3-37** and **Eq. 3-63**

	$\boldsymbol{T_1}$	$\boldsymbol{T_2}$	$\boldsymbol{T_3}$
$\boldsymbol{DTF(PDC)}$	0		
$\boldsymbol{gDTF}$	$S_{n,jj}^2 = \boldsymbol{\sigma}_{jj}^2$	$e_i^T(H\odot H^*)(\Sigma_e\odot\Sigma_e)(H\odot H^*)^T e_i$	$e_i^T(H\odot H^*)(\Sigma_e\odot\Sigma_e)e_j$
$\boldsymbol{iDTF}$		$\frac{e_i^T}{2}(H\Sigma_e H^T\odot H^*\Sigma_e H^H + H\Sigma_e H^H\odot H^*\Sigma_e H^T)e_i = \frac{1}{2}\left(\left\|\mu_{\gamma 1,i}\right\|^2 + \left\|\mu_{\gamma 2,i}\right\|^2\right)$	$e_i^T(H\Sigma_e\odot H^*\Sigma_e)e_j$
$\boldsymbol{gPDC}$	$S_{n,ii}^2 = \boldsymbol{\sigma}_{ii}^{-2}$	$e_j^T(B\odot B^*)^T S_n^2(\Sigma_e\odot\Sigma_e)S_n^2(B\odot B^*)e_j$	$\boldsymbol{\sigma}_{ii}^{-2}e_i^T(\Sigma_e\odot\Sigma_e)S_n^2(B\odot B^*)e_j$
$\boldsymbol{iPDC}$		$\frac{e_j^T}{2}\left(B^H{\Sigma_e}^{-1}B\odot B^T{\Sigma_e}^{-1}B^* + B^H{\Sigma_e}^{-1}B^*\odot B^T{\Sigma_e}^{-1}B\right)e_j = \frac{1}{2}\left(\left\|\mu_{\pi 1,j}\right\|^2 + \left\|\mu_{\pi 2,j}\right\|^2\right)$	$\boldsymbol{\sigma}_{ii}^{-2}e_i^T(B\odot B^*)e_j = \boldsymbol{\sigma}_{ii}^{-2}\|B_{ij}\|^2$

Confidence interval

Having the distribution of connectivity measures, the (1-α)% confidence interval is:

$$|\hat{\phi}_{ij}|^2 - z_{\alpha/2}\sqrt{\frac{\Omega_\phi}{n_s}} \le \left|\phi_{ij}\right|^2 \le \left|\hat{\phi}_{ij}\right|^2 + z_{\alpha/2}\sqrt{\frac{\Omega_\phi}{n_s}} \qquad \textbf{Eq. 3-64}$$

Confidence intervals of $|\gamma_{ij}|^2$ and $|\pi_{ij}|^2$ are obtained by inserting them in **Eq. 3-64** in the place of $|\phi_{ij}|^2$.

3.2.2 Asymptotic Distribution in Null Case

As mentioned in chapter three, according to [34] and [35], if H_0 holds, ($|\pi_{ij}|^2 = 0$ or $|\gamma_{ij}|^2 = 0$), the next term in the Taylor series in the *delta method* is important. They concluded that for large n_s, the distribution of $n_s\left(|\hat{\phi}_{ij}|^2 - |\phi_{ij}|^2\right)$ asymptotically converges to $Z^T \boldsymbol{D}\, Z$, where $Z \sim \mathcal{N}(0,1)$ with $\boldsymbol{D}$ being defined separately for the γ and π groups. Since $\boldsymbol{D}$ is a Hermitian matrix, it is diagonalizable: $Z^T \boldsymbol{D}\, Z = \sum_{k=1}^{q} \lambda_k Z^T v_k v_k^H Z$, where v_k is the k^{th} eigenvector of $\boldsymbol{D}$ associated with λ_k. Defining $\xi_k \triangleq v_k^H Z$ and since we know that $\xi_k \sim \mathcal{N}(0,1)$, $Z^T \boldsymbol{D}\, Z = \sum_{k=1}^{q} \lambda_k {\xi_k}^2$, which means that the distribution of $n_s\left(|\hat{\phi}_{ij}|^2 - |\phi_{ij}|^2\right)$ asymptotically converges to the linear combination of χ_1^2.

According to Patnaik approximation, the linear combination of the uncorrelated χ_1^2 random variables can be approximated by $c\chi_v^2$, where $\mathrm{c} = \sum_{k=1}^{q} l_k^2 / \sum_{k=1}^{q} l_k$, $v = \left(\sum_{k=1}^{q} l_k\right)^2 / \sum_{k=1}^{q} l_k^2$, and l_ks are multipliers [45]. By applying Patnaik approximation, they concluded:

$$n_s \phi_{d_{ij}}\left(|\hat{\phi}_{ij}|^2 - |\phi_{ij}|^2\right) \xrightarrow{d} c\chi_v^2 \qquad \textbf{Eq. 3-65}$$

where the multiplier *c* and the degree of freedom v are functions of the eigenvalues of $\boldsymbol{D}$. In the following sections, by explaining $\boldsymbol{D}_\pi$ and $\boldsymbol{D}_\gamma$ as a function of $L_{\overline{b}}$, $L_{\overline{h}}$, and estimating their dominant eigenvalues, *c* and *v* are found for both connectivity groups.

Statistical properties of group γ

For group γ, we obtained:

$$c = \lambda(1 + |R|^2) \qquad \textbf{Eq. 3-66}$$

$$v = \frac{2}{1 + |R|^2} \qquad \textbf{Eq. 3-67}$$

where λ is the product of the eigenvalues of $D_{\gamma,\Gamma}(j)$ and $D_{\gamma,e}(i)$:

$$D_{\gamma,\Gamma}(j) = \sigma_{jj}\{L_\Gamma^T(C^T \otimes H^*)(I_2 \otimes e_j)F_1(I_2 \otimes e_j^T)(C \otimes H^T)L_\Gamma\} \qquad \textbf{Eq. 3-68}$$

$$D_{\gamma,e}(i) = \left(HL_e(i)\right)^H HL_e(i) \qquad \textbf{Eq. 3-69}$$

$HL_e(i)$ is the i^{th} row of the HL_e, and R is the expected value of ${v_\Gamma}^T v_\Gamma \; {v_e}^T v_e$, where v_Γ and v_e are eigenvectors of $D_{\gamma,\Gamma}(j)$ and $D_{\gamma,e}(i)$, respectively.

Therefore, $D_{\gamma,e}(i)$ can be constructed in $O(K^3)$ operations and $D_{\gamma,\Gamma}(j)$ can be solved in $O(K^3p^2)$ operations including the multiplication of $(Kp \times 2)(2 \times 2)(2 \times Kp)$ inside the j loop, and building of the $(Kp \times Kp)$ matrix $L_\Gamma^T(C^T \otimes H^*)$ outside the j loop. According to **Appendix B.3**, finding v_Γ, v_e, λ requires $O(K^3p^2)$ operations which leads to overall $O(K^3p^2)$ calculations for estimating c and v.

- **Proof of Eq. 3-66 to Eq. 3-69:**

Applying the second term of Taylor series in *delta method* results that for large n_s, $n_s\left(|\hat{\gamma}_{ij}|^2 - |\gamma_{ij}|^2\right)$ converges to $X^T T_n \; X/\gamma_d$, where $X \sim \mathcal{N}(0, \Omega_{\overline{h}})$. If $X = L_{\overline{h}} Z$, then Z is a standard normal random variable, which yields $\boldsymbol{D}_\gamma = {L_{\overline{h}}}^T(T_n)L_{\overline{h}}$ [35].

By substituting T_n from Table 3-1 and Table 3-2, and $L_{\overline{h}}$ from **Eq. 3-7**, $\boldsymbol{D}_\gamma$ ($2K^2 \times 2K^2$matrix) can be rewritten as:

$$\boldsymbol{D}_{\gamma} = \Big\{\big\{{L_{\Gamma}}^{T}(\mathcal{C}^{T}F_1 \otimes H^{*})\big\} \otimes {L_e}^{T}H^{H} + \big\{{L_{\Gamma}}^{T}(\mathcal{C}^{T}F_2 \otimes H)\big\} \otimes {L_e}^{T}H^{T}\Big\}\big(I_2 \otimes E_j S_n \otimes E_i\big) \quad \textbf{Eq. 3-70}$$
$$\big\{\{(F_1\mathcal{C} \otimes H^{T})L_{\Gamma}\} \otimes HL_e + \{(F_2\mathcal{C} \otimes H^{H})L_{\Gamma}\} \otimes H^{*}L_e\big\}$$

So, $\boldsymbol{D}_{\gamma}$ is the summation of four terms, two of them are zero and the other nonzero terms are conjugate of each other:

$$\boldsymbol{D}_{\gamma} = \big\{{L_{\Gamma}}^{T}\big(\mathcal{C}^{T}F_1\mathcal{C} \otimes H^{*}E_j S_n H^{T}\big)L_{\Gamma}\big\} \otimes \big\{{L_e}^{T}H^{H}E_i H L_e\big\} + \big\{{L_{\Gamma}}^{T}\big(\mathcal{C}^{T}F_2\mathcal{C} \otimes HE_j S_n H^{H}\big)L_{\Gamma}\big\} \otimes \big\{{L_e}^{T}H^{T}E_i H^{*}L_e\big\} \quad \textbf{Eq. 3-71}$$

If $\boldsymbol{D}_{\gamma} \triangleq D + D^{*}$, where $D = D_{\gamma,\Gamma}(j) \otimes D_{\gamma,e}(i)$, $D_{\gamma,e}(i) = {L_e}^{T}H^{H}e_i{e_i}^{T}HL_e$ and $D_{\gamma,\Gamma}(j) = \sigma_{jj}\big\{{L_{\Gamma}}^{T}\big(\mathcal{C}^{T}F_1\mathcal{C} \otimes H^{*}e_j{e_j}^{T}H^{T}\big)L_{\Gamma}\big\}$. It is easy to show that the rank of D is one, and therefore, $rank\big(\boldsymbol{D}_{\gamma}\big) \leq 2\ rank(D) = 2$. Furthermore, D is a Hermitian, semi-positive definite matrix which has only one nonzero eigenvalue λ. Thus, $\boldsymbol{D}_{\gamma}$ can be rewritten as:

$$\boldsymbol{D}_{\gamma} = \lambda(\ v_1{v_1}^{H} + v_2{v_2}^{H}) \quad \textbf{Eq. 3-72}$$

v_1 and v_2 are respectively the eigenvectors of D and D^{*} associated with λ, and $v_2 = v_1^{*}$. Introducing $\xi_1 \triangleq v_1^{H}Z$ and $\xi_2 \triangleq v_2^{H}Z$ (we know that $\xi_2 \triangleq {\xi_1}^{*}$), then $Z^{T}\boldsymbol{D}_{\gamma}Z = \lambda\big({\xi_1}^{2} + {\xi_2}^{2}\big)$. $\xi_1$and ξ_2 are correlated and have asymptotic standard normal distribution. Defining the vector $\xi = [\xi_1, \xi_2]^{T}$, the covariance of ξ is:

$$cov(\xi) = \begin{bmatrix} 1 & cov(\xi_1, \xi_2) \\ cov(\xi_2, \xi_1) & 1 \end{bmatrix} \quad \textbf{Eq. 3-73}$$

where $cov(\xi_1, \xi_2)$ is defined:

$$cov(\xi_1,\xi_2) = E\left(\xi_1{\xi_2}^H\right) - E(\xi_1)E\left({\xi_2}^H\right) = E(v_1^H Z\ \ Z^T v_1^*) \\ = E(v_1^T v_1)^* \quad \textbf{Eq. 3-74}$$

If $R \triangleq cov(\xi_1,\xi_2)$, then $R^* \triangleq cov(\xi_2,\xi_1)$, and **Eq. 3-73** can be rewritten as:

$$cov(\xi) = \begin{bmatrix} 1 & R \\ R^* & 1 \end{bmatrix} \quad \textbf{Eq. 3-75}$$

$cov(\xi)$ is a Hermitian matrix with eigenvalues $1 \pm |R|$. The spectral decomposition of $cov(\xi)$ follows:

$$cov(\xi) = P\Lambda P^H \quad \rightarrow \quad P^H cov(\xi) P = \Lambda \quad \textbf{Eq. 3-76}$$

where $\Lambda = \begin{bmatrix} 1+|R| & 0 \\ 0 & 1-|R| \end{bmatrix}$, and unitary matrix $P = \frac{\sqrt{2}}{2}\begin{bmatrix} R/|R| & R/|R| \\ 1 & -1 \end{bmatrix}$. By applying Karhunen–Lo`eve expansion [46] and introducing $[u_1\ , u_2\ ]^T = P^H[\xi_1,\xi_2]^T$, we can conclude that $cov([u_1,u_2]) = P^H cov(\xi) P = \Lambda$. As Λ is a diagonal matrix, u_1 and u_2 are statistically independent. Also, $[\xi_1,\xi_2]^T = P[u_1\ , u_2\ ]^T$, so $\xi_1 = \frac{\sqrt{2}\,R}{2\,|R|}(u_1+u_2)$ and $\xi_2 = \frac{\sqrt{2}}{2}(u_1-u_2)$. Thus, $n_s\left(|\hat{\gamma}_{ij}|^2 - |\gamma_{ij}|^2\right)$ asymptotically converges to:

$$Z^T\ \boldsymbol{D}_\gamma Z = \lambda Z^T(u_1^H u_1 + u_2^H u_2)Z \quad \textbf{Eq. 3-77}$$

If $[\boldsymbol{u_1}, \boldsymbol{u_2}]$ is the standard form of $[u_1,u_2]$, then:

$$Z^T\ \boldsymbol{D}_\gamma Z = \lambda Z^T\left((1+|R|)\boldsymbol{u_1^H u_1} + (1-|R|)\boldsymbol{u_2^H u_2}\right)Z \quad \textbf{Eq. 3-78}$$

It can be concluded that $Z^T\ \boldsymbol{D}_\gamma Z \xrightarrow{d} c\chi_v^2$, where according to Patnaik approximation [45, 33], $c = \lambda(1+|R|^2)$ and $v = \frac{2}{1+|R|^2}$.

Furthermore, if eigenvectors of $D_{\gamma,\Gamma}(j)$ and $D_{\gamma,e}(i)$ are v_Γ and v_e, then $v_1 = v_\Gamma \otimes v_e$. Thus in **Eq. 3-74**:

$$R^* = E(v_1^T v_1) = E\left((v_\Gamma \otimes v_e)^T(v_\Gamma \otimes v_e)\right) = E({v_\Gamma}^T v_\Gamma\ {v_e}^T v_e) \quad \textbf{Eq. 3-79}$$

■

Statistical properties of group π

For group π, $\boldsymbol{D}_\pi = D_{\pi,\Gamma}(j) \otimes D_{\pi,e}(i)$, where $D_{\pi,\Gamma}(j) = L_\Gamma(j)^T\, \mathcal{C}^T \mathcal{C}\, L_\Gamma(j)$ and $D_{\pi,e}(i) = \sigma_{ii}^{-1} L_e(i)^T L_e(i)$. $L_e(i)$ (dimension of $1 \times K$) is the i^{th} row of the lower triangular matrix L_e, and $L_\Gamma(j)$ (dimension of $p \times Kp$) is the $(mK + j)^{th}$ rows of the lower triangular matrix L_Γ, for $(m = 0, \dots, p-1)$. Thus:

$$c = \left(\frac{\lambda_1^2 + \lambda_2^2}{\lambda_1 + \lambda_2}\right) \qquad \textbf{Eq. 3-80}$$

$$v = \frac{(\lambda_1 + \lambda_2)^2}{{\lambda_1}^2 + {\lambda_2}^2} \qquad \textbf{Eq. 3-81}$$

where λ_1 and λ_2 are the products of the eigenvalues of $D_{\pi,\Gamma}(j)$ and $D_{\pi,e}(i)$.

$D_{\pi,e}(i)$ and $D_{\pi,\Gamma}(j)$ can be solved in $O(K^3)$ and $O(K^3 p^2)$ operations, respectively, and with the same computational efforts for finding their eigenvalues. Since $D_{\pi,e}(i)$ is not frequency dependent, it can be estimated outside the loop. Finally, c and v are formed in $O(K^3 p^2)$ operations.

- **Proof of Eq. 3-80 and Eq. 3-81:**

According to [34] $\boldsymbol{D}_\pi = L_{\overline{b}}^{-T}(T_n) L_{\overline{b}}^{-}$. By substituting T_n from **Table 3-1** and **Table 3-2** and replacing $L_{\overline{b}}^{-}$ from **Eq. 3-5** , $\boldsymbol{D}_\pi$ ($2K^2 \times 2K^2$matrix) can be rewritten as:

$$\begin{aligned}
\boldsymbol{D}_\pi &= (L_\Gamma \otimes L_e)^T (\mathcal{C}^T \otimes I_{K^2}) \left(I_2 \otimes E_j \otimes E_i S_n\right) (\mathcal{C} \otimes I_{K^2}) (L_\Gamma \otimes L_e) \\
&= \left\{L_\Gamma{}^T (\mathcal{C}^T \otimes I_K) \left(I_2 \otimes E_j\right) (\mathcal{C} \otimes I_K) L_\Gamma\right\} \otimes \left\{L_e{}^T E_i S_n L_e\right\} \\
&= \left\{L_\Gamma{}^T \left(\mathcal{C}^T \mathcal{C} \otimes e_j e_j{}^T\right) L_\Gamma\right\} \otimes \left\{L_e{}^T e_i e_i{}^T S_n e_i e_i{}^T L_e\right\} \qquad \textbf{Eq. 3-82} \\
&= \left\{L_\Gamma{}^T \left(I_p \otimes e_j\right) \mathcal{C}^T \mathcal{C} \left(I_p \otimes e_j{}^T\right) L_\Gamma\right\} \otimes \left\{L_e(i)^T S_{n(ii)} L_e(i)\right\} \\
&= D_{\pi,\Gamma}(j) \otimes D_{\pi,e}(i)
\end{aligned}$$

Therefore, eigenvalues of $\boldsymbol{D}_{\pi}$ equal the multiplication of the eigenvalues of $D_{\pi,\Gamma}(j)$ and $D_{\pi,e}(i)$ which are semi-positive definite matrices with dimensions of $Kp \times Kp$, and $K \times K$, respectively. The ranks of $D_{\pi,\Gamma}(j)$ and $D_{\pi,e}(i)$ follow:

$$rank\big(D_{\gamma}(j)\ \big) \leq rank(C) = 2 \qquad \textbf{Eq. 3-83}$$

$$rank(D_{e}(i)\ ) = rank\big(L_{e}(i)\big) = 1 \qquad \textbf{Eq. 3-84}$$

Since $rank(\boldsymbol{D}_{\pi}) = rank(D_{\pi,\Gamma}(j)\ \times D_{\pi,e}(i)\ )$, then $rank(\boldsymbol{D}_{\pi}) \leq 2$. Hence, $\boldsymbol{D}_{\pi}$ has at most two positive eigenvalues, while the remaining eigenvalues are zero. Finally, c and v are obtained by applying the Patnaik approximation [45, 33]. ■

3.3 Computational Complexity of Fast Asymptotic Algorithm

The fast asymptotic algorithm can be divided into two major parts in terms of dependency on frequency. Reducing the workload in the frequency loop is particularly valuable when it is required to be run on a wide range of frequencies. In the proposed algorithm, the Cholesky decomposition which is a significant source of work -perhaps the dominant one- is executed outside the frequency loop.

The frequency-dependent computational efforts consist of two consecutive steps; null and non-null case. The source of work on the null case is to solve the eigenvalue/eigenvector problem, and the source work on the non-null case is the matrix-matrix multiplication. Furthermore, the non-null case is performed in the case of rejection of the null hypothesis.

In general, the computational complexity of the whole algorithm except for calculating the Γ_{y}^{-1} is independent of n_s. The computational cost of each part as a function of K and

p is evaluated according to **Appendix B** and the final assessments are provided in **Table 3-5**. According to **Table 3-5**, the total procedure over one frequency is $O(K^3p^3)$.

Table 3-5: Time complexity of the Fast Asymptotic algorithm

	PROCEDURE		**TIME COMPLEXITY**	
			GROUP π	GROUP γ
Outside frequency loop	Cholesky decomposition of Σ_e		$O(K^3)$	
	Building Γ_y^{-1}		$O(n_sK^2p^2 + K^3p^3)$	
	Cholesky decomposition of Γ_y^{-1}		$O(K^3p^3)$	
Inside frequency loop	Estimating $\lvert\phi_{ij}\rvert^2$		$O(K^3 + K^2p)$ for $iPDC$ and $iDTF$ $O(K^2p)$ for other measures	
	Null case	Eigenpairs of $D_{\phi,\Gamma}$	$O(K^3p^2)$	$O(K^3p^2)$
		Eigenpairs of $D_{\phi,e}$	$O(K^3)$(outside frequency loop)	$O(K^3)$
	Non-null case	Ω_{ϕ_σ}	$O(K^3)$	$O(K^3)$
		$\Omega_{\phi_{(\bar{h}\ or\ \bar{b})}}$	$O(K^3 + Kp^2)$	$O(K^3p^2)$

CHAPTER 4

PERFORMANCE EVALUATION OF THE PROPOSED FAST ASYMPTOTIC METHODOLOGY

4.1 Validation of the Fast Asymptotic Algorithm

We first validated the results on connectivity statistics from our new fast asymptotic algorithm by comparing them with the ones from the original asymptotic algorithm in a well-cited simulation example in the literature [16, 35]. The equations of the investigated 5-dimensional, 2nd order, interconnected system, are the following:

$$
\begin{aligned}
y_1(n) &= 0.95\sqrt{2}\,y_1(n-1) - 0.9025\,y_1(n-2) + 0.5\,y_5(n-2) + \boldsymbol{\epsilon}_1(n)\\
y_2(n) &= -0.5\,y_1(n-1) + \boldsymbol{\epsilon}_2(n)\\
y_3(n) &= 0.4\;y_2(n-2) + \boldsymbol{\epsilon}_3(n)\\
y_4(n) &= -0.5\;y_3(n-1) + 0.25\sqrt{2}\,y_4(n-1) + 0.25\sqrt{2}\,y_5(n-1) + \boldsymbol{\epsilon}_4(n)\\
y_5(n) &= -0.25\sqrt{2}\,y_4(n-1) + 0.25\sqrt{2}\,y_5(n-1) + \boldsymbol{\epsilon}_5(n)
\end{aligned}
\qquad \textbf{Eq. 4-1}
$$

Figure 4-1 illustrates the direct connectivity diagram of **Eq. 4-1**. According to **Figure 4-1**, signals from any structure can reach all other structures. The diagram shows the existence of the direct coupling between consecutive signals. Moreover, $y_5(n)$ is a direct source to $y_1(n)$ and $y_4(n)$.

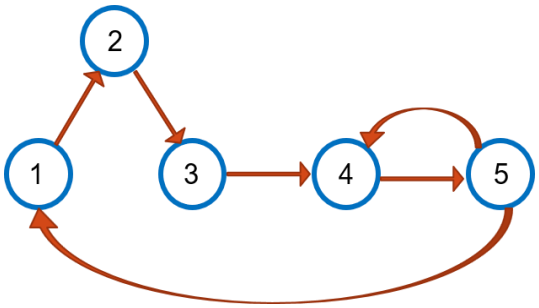

Figure 4-1: Connectivity diagram between all structures for **Eq. 4-1**.

The connectivity results from the application of the original and new algorithm to the estimation of the statistics of $iPDC$ and $iDTF$ measures in the $\boldsymbol{y}(n)$ signals generated from system **Eq. 4-1**, using standard white noise processes for $\boldsymbol{\epsilon}(n)$ and with $n_s = 2000$, $\alpha = 0.01,$ are shown in **Figure 4-2** and **Figure 4-3** respectively. It is shown that the statistical thresholds and confidence intervals for the estimated connectivity measures between the system's $\boldsymbol{y}(n)$ variables by the proposed fast asymptotic algorithm were identical to the ones from the original asymptotic algorithm reported in [16, 35].

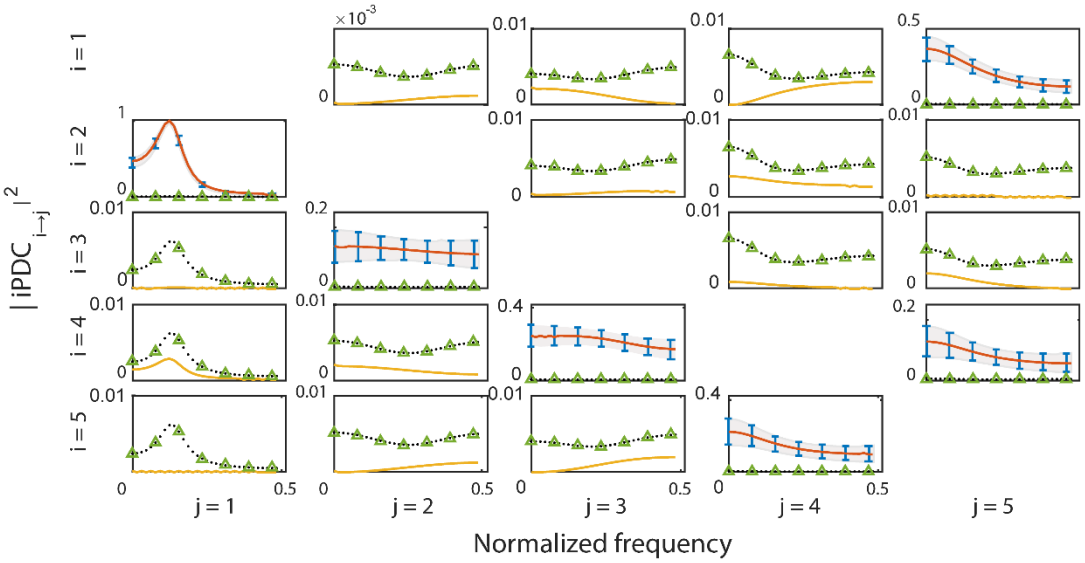

Figure 4-2: Comparative statistics from the original and the new asymptotic estimation of the $iPDC(f)$ connectivity measures for **Eq. 4-1**. The statistical threshold is denoted by black dashed lines if estimated by the original algorithm, and with green triangle

symbols if estimated by the new algorithm. The 99% confidence interval is denoted by error bars, gray for the original, and blue for the proposed algorithms. Indexes ***i*** and ***j*** are denoting the sinks and sources, respectively.

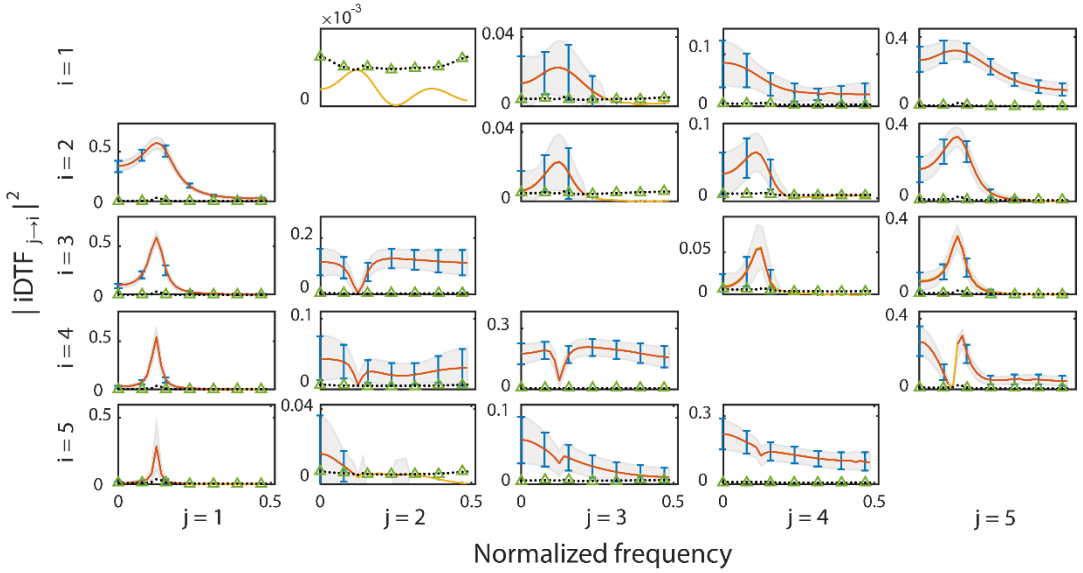

Figure 4-3: Comparative statistics from the original and the new asymptotic estimation of the $iDTF(f)$ measures for **Eq. 4-1** . The statistical threshold is denoted by black dashed lines if estimated by the original algorithm, and with green triangle symbols if estimated by the new algorithm. The 99% confidence interval is denoted by error bars, gray for the original, and blue for the proposed algorithms. Indexes ***i*** and ***j*** are denoting the sinks and sources, respectively.

4.2 Use of Asymptotic Versus Surrogate Statistics

In the same simulation experiment, we then compared the results from the asymptotic methodology to the ones from the surrogate methodology denoted as causal Fourier transform shuffling (CFT) for estimation of the statistics of the derived connectivity measures (shown in **Figure 4-4**). We figured out that the results obtained from both statistical methods completely match for the connectivities in group π which is in agreement with[21]. It is shown that the use of CFT surrogates provides false information about causal coupling between some of the system's variables in group γ. In

particular, from **Figure 4-4**, we can see that the 99% threshold obtained by CFT for $|\gamma_{2,3}(f)|^2$, $|\gamma_{3,4}(f)|^2$ and $|\gamma_{5,2}(f)|^2$ does not match the one from the asymptotic theory, which results in false conclusions about the statistical significance of the estimated connectivities, especially the 3⟶2 connectivity over a wide spectral band.

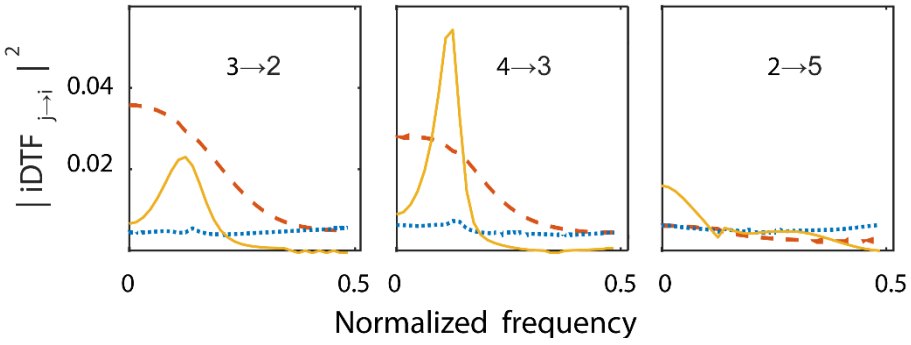

Figure 4-4: The connectivity measure $|iDTF|^2$ estimated from signals generated by the simulation example **Eq. 4-1** and its statistical 99% thresholds over frequency obtained by a) the CFT method and 100 surrogates (dashed red lines) and b) by the new asymptotic theory (blue dotted lines). The asymptotic methods provide more accurate statistically significant values for the actual connectivities than the surrogate method. Note: The threshold values with the new are the same as with the original asymptotic theory (see **Figure 4-3**).

4.3 Computation Time of the Fast Versus the Original Asymptotic Algorithm

Intracranial EEG (iEEG) recordings consented at the U. Alabama's medical center was used for comparison of the original and the new asymptotic methods with respect to the computation time required for estimation of ϕ connectivity measures.

Figure 4-5 shows the computation time for the original and the new asymptotic algorithms for 10 sec EEG segments recorded concurrently from K $(K = 2,..,32)$ electrodes and with sampling frequency $f_s = 500$ Hz (that is, $n_s = 5000$ data points per electrode / dimension). Both algorithms ran on a computer with a 2.2 GHz Intel Xeon processor and 128 GB of RAM. They were written in MATLAB, and the function

"$timeit$" was used to measure the median of computation time for the estimation of the asymptotic statistics of $iDTF$ and $iPDC$ connectivity measures at one frequency ($f = 41$ Hz) per algorithm. For estimation of computation time, the algorithm was forced to run both null and non-null cases. The computation time of the proposed algorithm as a function of p is visibly shorter than the original one (**Figure 4-5**, right panels). More importantly, a clear exponential increase of computation time of the original algorithm with K is apparent (**Figure 4-5**, left panels).

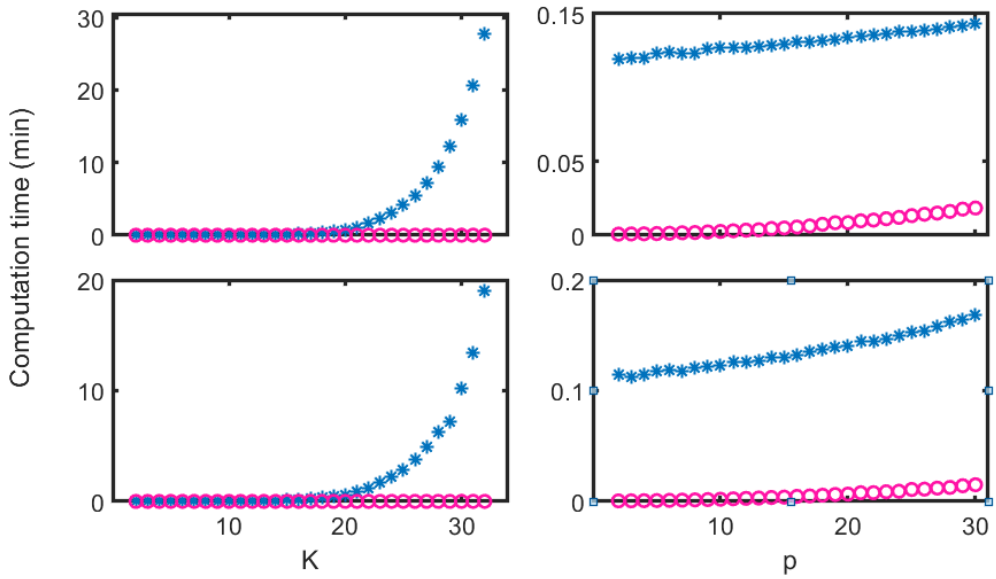

Figure 4-5: Computation time (min) of "$iDTF$" (top panels) and "$iPDC$" (bottom panels) of the original algorithm (blue asterisk $*$) and the proposed algorithm (red circle o) versus K (left) for $p = 3$, and versus p (right) for $K = 15$. The algorithms were applied to EEG datasets of 10 sec in duration ($f_s = 500$ Hz) and $iDTF$ and $iPDC$ were estimated at a single frequency ($f = 41$ Hz).

Having shown the superiority of the new asymptotic algorithm over the original one with respect to computation time required for the estimation of ϕ measures of connectivity, we sought to further investigate the effect of larger values of K and p on the computation time of the proposed new algorithm. In **Figure 4-6**, the computation time of

the six different connectivity measures discussed in this study was estimated. According to the left panel of **Figure 4-6**, when $p = 3$, real-time (10 sec, i.e. approximately 0.16 minutes) computation for the group π of ϕ connectivity measures (PDC, $gPDC$ and $iPDC$) is achieved with dimension K less than 500, and for the group γ (DTF, $gDTF$ and $iDTF$) with dimension K less than 330. Our investigation indicates that the computation time for estimation of all ϕ connectivity measures depends on p in an identical way. Therefore, we plot only $iPDC$ and $iDTF$ in the right panel of **Figure 4-6**, from which we can conclude that, with $K = 15$, the computation of ϕ connectivity measures is achieved in real time with model order p less than 75.

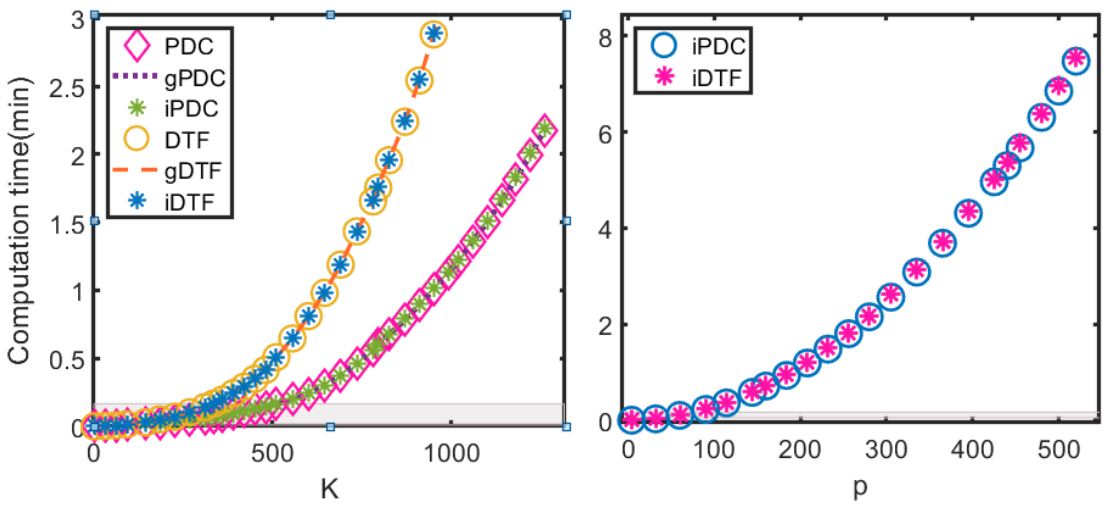

Figure 4-6: Computation time (min) for estimation of the statistics of connectivity measures versus K and p. *Left panel:* Computation time of all measures versus K with $p = 3$ [PDC (diamond), $gPDC$ (dotted lines), $iPDC$ (green asterisk), DTF (circle), $gDTF$ (dashed line), and $iDTF$ (blue asterisk)]. *Right panel:* Computation time versus p with $K = 15$ for $iPDC$ (circle) and $iDTF$ (asterisk). $f_s = 2000$ Hz and $f = 41$ Hz. Runtimes of the connectivity measures as functions of K are very similar within group π or group γ; they are almost identical across groups with respect to p.

The order of complexity of the proposed algorithm is illustrated by the log-log plot of **Figure 4-6.** Since the computation time of the connectivity measures within each

group is almost identical when analyzed with respect to K, and is nearly equal for both groups in evaluations versus p, in **Figure 4-7,** we just investigated the $iPDC$ and $iDTF$ in the logarithmic plots**.**

In **Figure 4-7,** the tangential lines fitted to $iPDC$ and $iDTF$ curves are almost parallel with the approximate slope of 2.7 for K (left). Furthermore, the tangential line fitted to $iDTF$ has the slope of 2.05 for p (right). The results are consistent with the order of complexities obtained in chapter three.

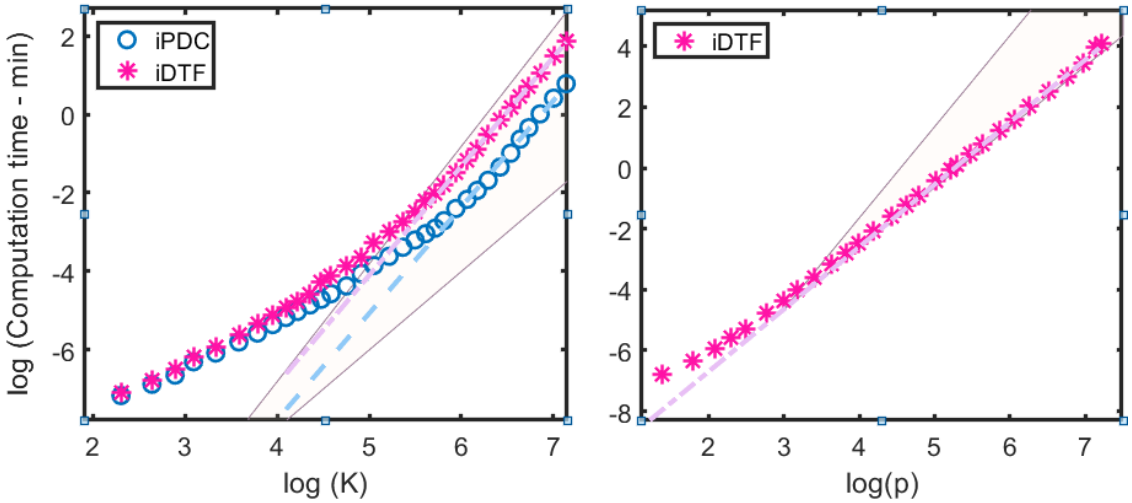

Figure 4-7: Log of computation time (min) of $iPDC$ (circle) and $iDTF$(asterisk) versus natural logarithm of K (left) for $p = 3$, and versus natural logarithm of p (right) for $K = 15$. The dashed lines are fitted on curves for $K > 340$ with the approximate slope of 2.7 (left graph), and for $p > 280$ with the approximate slope of 2.05 (right graph). The shaded area represents the minimum slope of 2 and the maximum slope of 3. The algorithms were applied to EEG datasets of 10 sec in duration ($f_s = 2000$ Hz) and $iDTF$ and $iPDC$ were estimated at a single frequency ($f = 41$ Hz).

The remarkable potential of the proposed algorithm to deal with a wide range of frequencies is shown in **Figure 4-8**. According to **Figure 4-8**, the new algorithm noticeably consumes less computation time (solid lines) than expected (dotted lines), especially for $iPDC$, when it runs over a wide frequency range.

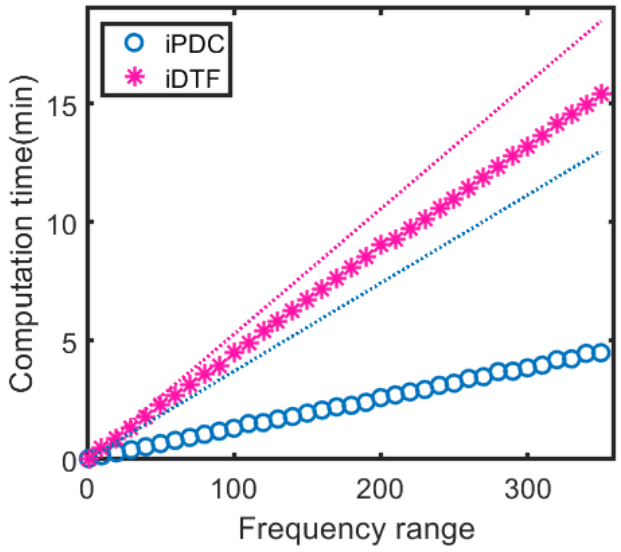

Figure 4-8: Computation time (min) of $iPDC$ (circle) and $iDTF$(asterisk) as a function of number of frequencies the measures are estimated at. The algorithm was applied to 10 sec EEG datasets of a patient with 122 electrodes ($K = 122$), where the model order $p = 8$ was determined using Akaike's information criterion. The dotted lines (blue for $iPDC$ and pink for $iDTF$) represent the expected computation time when the algorithm runs for each single frequency.

CHAPTER 5

CONCLUSION AND FUTURE WORK

5.1 Conclusion

In this study, we addressed a substantial drawback in the application of the published asymptotic MVAR method to the estimation of statistically significant causal connectivity measures in high-dimensional time series. It has been previously shown [21] that the asymptotic method provides shorter computation time than the one of empirical approaches that use surrogate data such as CFT [28]. Although the original asymptotic algorithms first delineated in [34] and [35] are fast when compared with surrogate methods, they are not fast enough to be applied to high-dimensional time series. We proposed a new methodology to address this drawback that required extensive changes in the formulation of the original methodology. In chapter three, it was shown that the proposed algorithm can be accomplished using $O(K^3p^3)$ operations. It is also noteworthy that the ratio of the computation time of the new algorithm over the computation time of the original asymptotic algorithm decreases exponentially with the dimension K (approximately $\exp(-0.2K)$, for $K = 2, \ldots, 32$; see **Figure 4-5**).

The major modifications we performed include:

1) Decrease the dimensions of the involved matrices by implementing the properties of vec operator (**Appendix A.1**). These transformations dismissed the redundant Kronecker products, "diag" operators, and, when combined with **Eq. 3-11**, discard the commutation matrix.

2) Separate $i, j,$ and f variables in the involved equations as this decreases the computational complexity due to loops.

3) Simplify the estimation of the gradient of connectivity measures ϕ by appropriate reformatting of the involved equations. As explained in chapter three, part 3.2.1, for computing the covariance of ϕ with respect to $\boldsymbol{\sigma}$, instead of equations in **Table 2-2** and **Table 2-3** used in the original algorithm, separable equations are applied. This simple change in the new algorithm resulted in dealing with matrices of dimension of order K instead of K^4.

4) In the original asymptotic algorithm, the Cholesky factorization of $\Omega_{\bar{b}}$ (or $\Omega_{\bar{h}}$) with dimension of $2K^2 \times 2K^2$ has to be performed for each frequency. However, in the new algorithm, factorization of Γ_y^{-1} (with dimension of $Kp \times Kp$) and Σ_e(with dimension of $K \times K$) is done once and it can then be used in the estimations at all frequencies. $\Omega_{\bar{b}}$ (or $\Omega_{\bar{h}}$) was decomposed according to **Eq. 3-5** and **Eq. 3-7**. By considering the complexity of Cholesky factorization (**Appendix B.2**), this modification leads to a remarkable improvement in the speed of the algorithm.

5) Speed up the finding of the dominant eigenvalues. By decomposing the matrices ($\boldsymbol{D}_\pi$ or $\boldsymbol{D}_\gamma$) and applying the powerful properties of Kronecker product, we reduced the size of the matrices in the related characteristic polynomial from $2K^2 \times 2K^2$ to two low-dimensional matrices with the size of $K \times K$ and $Kp \times Kp$.

6) Separation of the variables in $\boldsymbol{D}_{PDC}$ (or $\boldsymbol{D}_{DTF}$) in terms of i and j for each frequency f, also helped the required instructions to run on $2K$ loops instead of K^2 loops, a huge improvement.

7) The effect on complexity of matrix multiplication does not seem to be noticeable, unless we deal with extremely high-dimensional matrices (**Appendix B.1)**. In the new algorithm, due to decrease in the dimension of matrices, the complexity of multiplication of high-dimensional matrices is significantly reduced. The modification in **Eq. 3-4**, and the matrix form representation of $\mathcal{H}$ in **Eq. 3-6** were prerequisites for these improvements.

We validated the new asymptotic MVAR method with a simulation example. Considering the extensive applications of the connectivity measures for the analysis of a plurality of other high-dimensional biological signals in real-time, availability of fast asymptotic MVAR algorithms like the one we herein present is critical for generation of timely and reliable results.

5.2 Future Work

Substantial optimization of the asymptotic algorithm performed in this thesis facilitates a practical algorithm for high-dimensional time series of real-life instances. Hence, applying the proposed algorithm on a physiological example with high-dimensional physiological time series such as EEG is crucial to show the need for the new than the original methodology to accurately address a clinical problem.

APPENDIX A

MATRIX PROPERTIES [44]

A.1 Vectorization Operator (vec)

If X, A, B, C, and D are matrices with the dimensions of $(m \times n)$, $(p \times m)$, $(n \times q)$, $(p \times q)$, and $(q \times m)$ respectively, Y, and Z are $(m \times m)$ matrices, and x is a m-dimensional vector, some of the properties of the column vectorizing operator, vec, which were implemented in this study are as follows:

$$\frac{\partial vec(AXB)}{\partial vec(X)^T} = B^T \otimes A \qquad \textbf{Eq. A-1}$$

$$vec(X)^T (B \otimes A^T) = vec(AXB)^T \qquad \textbf{Eq. A-2}$$

$$\text{If } A = CD \quad \rightarrow \quad vec(A) = \left(D^T \otimes I_p\right) vec(C) \qquad \textbf{Eq. A-3}$$

$$\frac{\partial (x^T C x)}{\partial vec(x)} = x(C + C^T) \qquad \textbf{Eq. A-4}$$

For nonsingular Y: $$\frac{\partial vec(Y^{-1})}{\partial vec(Y)} = -Y^{-T} \otimes Y^{-1} \qquad \textbf{Eq. A-5}$$

$$\frac{\partial vec(Y \odot Z)}{\partial vec(Y)} = diag(vec(Z)) \qquad \textbf{Eq. A-6}$$

$$vec(D^T)^T (C^T \otimes X) vec(B) = trace(XBCD) = trace(DXBC) = trace(CDXB) = trace(BCDX) \qquad \textbf{Eq. A-7}$$

A.2 Rank of Matrix ($\boldsymbol{rank}$)

Rank of a matrix is the maximum number of linearly independent rows or columns of the matrix. Here, some general properties of the $\boldsymbol{rank}$ function exploited in this study are presented. For three matrices A, B, and C with the dimensions of $(m \times n)$, $(n \times r)$, and $(m \times n)$, respectively:

$$rank(AB) \leq \min\{rank(A), rank(B)\} \quad \textbf{Eq. A-8}$$

$$rank(A \otimes B) = rank(A)rank(B) \quad \textbf{Eq. A-9}$$

$$rank(A + C) \leq rank(A) + rank(C) \quad \textbf{Eq. A-10}$$

$$rank(A^*) = rank(A) = rank(A^H) \quad \textbf{Eq. A-11}$$

A.3 Moore-Penrose Pseudo-inverse

The Moore-Penrose pseudo-inverse of $(m \times n)$ matrix A is the unique matrix A^+ with a dimension of $(n \times m)$ satisfying the four Moore-Penrose conditions:

$$1.\ AA^+A = A, \qquad 2.\ A^+AA^+ = A^+,$$
$$3.\ (AA^+)^H = AA^+, \quad 4.\ (A^+A)^H = A^+A \quad \textbf{Eq. A-12}$$

If $A = USV^H$ is the Singular Value Decomposition (SVD) of A with $r = rank(A)$, and $s_1, s_2, \ldots, s_r$ being the nonzero elements lie along the main diagonal of S, then $A^+ = VS^+U^H$, where S^+ is a $(n \times m)$ diagonal matrix with $\frac{1}{s_1}, \frac{1}{s_2}, \ldots, \frac{1}{s_r}$ being the components of the main diagonal.

A.4 Commutation Matrix

$T_{m,n}$ is called the commutation matrix with a dimension of $(mn \times mn)$ such that for matrix A with a dimension of $(m \times n)$, $vec(A^T) = T_{m,n}vec(A)$.

If A is a $(m \times m)$ symmetric matrix, then according to the definition:

$$T_{m,m}vec(A) = vec(A) \rightarrow T_{m,m} = I_{m^2} \quad \textbf{Eq. A-13}$$

If D_m is a Duplication matrix with a dimension of $\left(m^2 \times 1/2\, m(m+1)\right)$, then:

$$D_m D_m^+ = \frac{1}{2}\left(I_{m^2} + T_{m,m}\right) \quad \textbf{Eq. A-14}$$

A.5 Kronecker Product (denoted by ⊗) Properties:

If A, B, C, D, and E are $(m \times n)$, $(p \times q)$, $(n \times r)$, $(q \times s)$, and $(p \times q)$ dimension matrices, respectively, the following rules of the Kronecker products hold:

$$(A \otimes B)(C \otimes D) = AC \otimes BD \quad \textbf{Eq. A-15}$$

$$A \otimes (B \pm E) = A \otimes B \pm A \otimes E \quad \textbf{Eq. A-16}$$

$$(A \otimes B)^H = A^H \otimes B^H\ ,\ (A \otimes B)^T = A^T \otimes B^T\ ,\ (A \otimes B)^* = A^* \otimes B^* \quad \textbf{Eq. A-17}$$

For A and B being square matrices, if $\lambda(A)$ and $\lambda(B)$ are the vectors containing the eigenvalues of A and B with associated eigenvectors $v(A)$ and $v(B)$, then:

$$\lambda(A \otimes B) = \lambda(A) \otimes \lambda(B) \quad \textbf{Eq. A-18}$$

$$v(A \otimes B) = v(A) \otimes v(B) \quad \textbf{Eq. A-19}$$

A.6 Spectral Decomposition of a Hermitian Matrix

The Hermitian $(n \times n)$ matrix A is diagonalizable in the form of $A = U\Lambda U^H$, where U is a unitary matrix whose columns are the orthonormal eigenvectors of A associated with eigenvectors $\lambda_1, \lambda_2, \ldots, \lambda_n$, and $\Lambda = diag\ (\lambda_1, \lambda_2, \ldots, \lambda_n)$.

APPENDIX B

COMPLEXITY OF THE IMPLEMENTED FUNCTIONS

B.1 Matrix Multiplication and Inversion

The computation of conventional matrix-matrix multiplication is $O(n^3)$. By applying fast multiplication algorithms, the computation can be done with less arithmetic. For instance, the Strassen's method is $O(n^{2.807})$ and Coppersmith-Winograd algorithm which is the fastest currently known algorithm is $O(n^{2.376})$. Strassen's method appears in the libraries like BLAS (Basic Linear Algebra Subprograms) where $n > \sim 100$.

The complexity for estimating the matrix inversion is $O(n^3)$ when algorithms such as Gauss-Jordan, LU decomposition, Gaussian elimination are applied. However, Strassen and Coppersmith-Winograd methods acquire the same complexity in matrix inversion as in matrix multiplication [47].

Matrix operations on MATLAB built on LAPACK (Linear Algebra Package), use the optimized block matrix algorithms that operate on several columns of a matrix at a time. On machines with high-speed cache memory, these algorithms can considerably accelerate the computations involving large matrices by factors of two to eight [48].

In this study, to estimate the computational complexity of the proposed algorithm, we assumed the worst-case computation of matrix-matrix multiplication and inversion of $O(n^3)$ and Kronecker product of $O(n^4)$.

B.2 Cholesky Decomposition

The Hermitian positive definite $(n \times n)$ matrix A has a special factorization called "Cholesky decomposition". According to this factorization, A can be decomposed to the

product of the unique lower triangle matrix L and its conjugate transpose, L^H. The "Cholesky factor" L, sometimes is referred to as the square root of A, albeit literally it is not.

The elements of $L = l_{ij}$ are given as:

$$l_{ii} = \sqrt{a_{ii} - \sum_{k=0}^{i-1} l_{ik}^2} \qquad \textbf{Eq. B-1}$$

$$\boldsymbol{l_{ij} = \frac{1}{l_{jj}}\left(a_{ij} - \sum_{k=0}^{j-1} l_{ik} l_{jk}\right) \quad j < i} \qquad \textbf{Eq. B-2}$$

According to **Eq. B-1** and **Eq. B-2**, L can be built by estimating the main diagonal with $n\,(n-1)/2$ multiplications and n square roots, and the other lower triangular elements by $n\,(n-1)(n-2)/6$ multiplications and $n\,(n-1)/2$ divisions. As a result, the operations count for estimating the Cholesky factor is $O(n^3)$ [47].

B.3 Eigen-pair Calculation

In this study, the MATLAB function "eigs" was used to find a few, say k, dominant eigenvalues and their associated eigenvectors of a n-dimensional Hermitian matrix. "Implicit restarting Lanczos Method" defined in ARPACK (Arnoldi Package) software is used in MATLAB to implement the "eigs" function.

This method executes efficiently by restricting the maximum number of steps in the Lanczos process, and subsequently leads to fewer arithmetic operations and storage ($2nk + O(k^2)$ storage). The computational complexity of this method is determined through matrix-vector products with the worst case being $O(n^2)$ [49, 50].

BIBLIOGRAPHY

1. Faes, Luca, Silvia Erla, and Giandomenico Nollo. "Measuring connectivity in linear multivariate processes: definitions, interpretation, and practical analysis." *Computational and mathematical methods in medicine* 2012 (2012).

2. Vlachos, Ioannis, et al. "The concept of effective inflow: application to interictal localization of the epileptogenic focus from iEEG." *IEEE Transactions on Biomedical Engineering* 64, no. 9 (2016): 2241-2252.

3. Lehnertz, Klaus. "Assessing directed interactions from neurophysiological signals-an overview." *Physiological measurement* 32, no. 11 (2011): 1715-24.

4. Britton, JeffreyW., et al. *Electroencephalography (EEG): An introductory text and atlas of normal and abnormal findings in adults, children, and infants*. American Epilepsy Society, Chicago, 2016.

5. Malmivuo, Jaakko, and Robert Plonsey. *Bioelectromagnetism: principles and applications of bioelectric and biomagnetic fields*. Oxford University Press, USA, 1995.

6. Franaszczuk, Piotr J., Gregory K. Bergey, and M. J. Kaminski. "Analysis of mesial temporal seizure onset and propagation using the directed transfer function method." *Electroencephalography and clinical neurophysiology* 91, no. 6 (1994): 413-427.

7. Gersch, Will, and G. V. Goddard. "Epileptic focus location: spectral analysis method." *Science* 169, no. 3946 (1970): 701-702.

8. Lu, Yunfeng, et al. "Seizure source imaging by means of FINE spatio-temporal dipole localization and directed transfer function in partial epilepsy patients." *Clinical Neurophysiology* 123, no. 7 (2012): 1275-1283.

9. Ding, Lei, et al. "Ictal source analysis: localization and imaging of causal interactions in humans." *Neuroimage* 34, no. 2 (2007): 575-586.

10. Kamiński, Maciej, Katarzyna Blinowska, and Waldemar Szelenberger. "Topographic analysis of coherence and propagation of EEG activity during sleep and wakefulness." *Electroencephalography and clinical neurophysiology* 102, no. 3 (1997): 216-227.

11. Blinowska, Katarzyna, et al. "Transmission of brain activity during cognitive task." *Brain topography* 23, no. 2 (2010): 205-213.

12. Babiloni, Claudio, et al. "Directionality of EEG synchronization in Alzheimer's disease subjects." *Neurobiology of aging* 30, no. 1 (2009): 93-102.

13. Varotto, Giulia, et al. "Enhanced frontocentral EEG connectivity in photosensitive generalized epilepsies: a partial directed coherence study." *Epilepsia* 53, no. 2 (2012): 359-367.

14. Granger, Clive WJ. "Time series analysis, cointegration, and applications." *American Economic Review* 94, no. 3 (2004): 421-425.

15. Hlaváčková-Schindler, Katerina, et al. "Causality detection based on information-theoretic approaches in time series analysis." *Physics Reports* 441, no. 1 (2007): 1-46.

16. Baccalá, Luiz A., and Koichi Sameshima. "Partial directed coherence: a new concept in neural structure determination." *Biological cybernetics* 84, no. 6 (2001): 463-474.

17. Kamiński, Maciej, et al. "Evaluating causal relations in neural systems: Granger causality, directed transfer function and statistical assessment of significance." *Biological cybernetics* 85, no. 2 (2001): 145-157.

18. He, Bin, et al. "Electrophysiological brain connectivity: theory and implementation." *IEEE transactions on biomedical engineering* 66, no. 7 (2019): 2115-2137.

19. Kaminski, Marcin Jan, and Katarzyna J. Blinowska. "A new method of the description of the information flow in the brain structures." *Biological cybernetics* 65, no. 3 (1991): 203-210.

20. Sameshima, Koichi, and Luiz Antonio Baccala, eds. *Methods in brain connectivity inference through multivariate time series analysis*. CRC press, 2014.

21. Toppi, Jlenia, et al. "Testing the significance of connectivity networks: Comparison of different assessing procedures." *IEEE Transactions on Biomedical Engineering* 63, no. 12 (2016): 2461-2473.

22. Moharramipour, Ali, et al. "Comparison of statistical tests in effective connectivity analysis of ECoG data." *Journal of Neuroscience Methods* 308 (2018): 317-329.

23. Whitley, Elise, and Jonathan Ball. "Statistics review 6: Nonparametric methods." *Critical care* 6, no. 6 (2002): 509.

24. Schlögl, Alois, and Gernot Supp. "Analyzing event-related EEG data with multivariate autoregressive parameters." *Progress in brain research* 159 (2006): 135-147.

25. Florin, Esther, et al. "Reliability of multivariate causality measures for neural data." *Journal of neuroscience methods* 198, no. 2 (2011): 344-358.

26. Efron, Bradley. "Nonparametric estimates of standard error: the jackknife, the bootstrap and other methods." *Biometrika* 68, no. 3 (1981): 589-599.

27. Lancaster, Gemma, et al. "Surrogate data for hypothesis testing of physical systems." *Physics Reports* 748 (2018): 1-60.

28. Faes, Luca, Alberto Porta, and Giandomenico Nollo. "Testing frequency-domain causality in multivariate time series." *IEEE transactions on biomedical engineering* 57, no. 8 (2010): 1897-1906.

29. Faes, Luca, et al. "Surrogate data analysis for assessing the significance of the coherence function." *IEEE transactions on biomedical engineering* 51, no. 7 (2004): 1156-1166.

30. Prichard, Dean, and James Theiler. "Generating surrogate data for time series with several simultaneously measured variables." *Physical review letters* 73, no. 7 (1994): 951.

31. Van der Vaart, Aad W. *Asymptotic statistics*. Vol. 3. Cambridge university press, 2000.

32. Schelter, Björn, et al. "Testing for directed influences among neural signals using partial directed coherence." *Journal of neuroscience methods* 152, no. 1-2 (2006): 210-219.

33. Yasumasa Takahashi, Daniel, Luiz Antonio Baccal, and Koichi Sameshima, "Connectivity inference between neural structures via partial directed coherence." *Journal of Applied Statistics* 34, no. 10 (2007): 1259-1273.

34. Baccalá, Luiz A., et al. "Unified asymptotic theory for all partial directed coherence forms." *Philosophical Transactions of the Royal Society A: Mathematical, Physical and Engineering Sciences* 371, no. 1997 (2013): 1-13.

35. Baccalá, Luiz A., Daniel Y. Takahashi, and Koichi Sameshima, "Directed transfer function: Unified asymptotic theory and some of its implications." *IEEE Transactions on Biomedical Engineering* 63, no. 12 (2016): 2450-2460.

36. Georgis, Georgios, et al. "Neuronal connectivity assessment for epileptic seizure prevention: Parallelizing the generalized partial directed coherence on many-core platforms." In *2014 International Conference on Embedded*

Computer Systems: Architectures, Modeling, and Simulation (SAMOS XIV), pp. 359-366. IEEE, 2014.

37. Akaike, Hirotugu. "On the use of a linear model for the identification of feedback systems." *Annals of the Institute of statistical mathematics* 20, no. 1 (1968): 425-439.

38. Saito, Y., and H. Harashim. "Tracking of information within multichannel EEG record-casual analysis in EEG." *Recent advances in EEG and EMG data processing*, pp. 133-146, Elsevier/North-Holland, Amsterdam, 1981.

39. Baccalá, L.A., et al. "Studying the interaction between brain structures via directed coherence and Granger causality." *Applied signal processing* 5, no. 1 (1998): 40.

40. Schelter, Björn, Jens Timmer, and Michael Eichler. "Assessing the strength of directed influences among neural signals using renormalized partial directed coherence." *Journal of neuroscience methods* 179, no. 1 (2009): 121-130.

41. Takahashi, Daniel Y., Luiz A. Baccalá, and Koichi Sameshima. "Information theoretic interpretation of frequency domain connectivity measures." *Biological cybernetics* 103, no. 6 (2010): 463-469.

42. Baccalá, Luiz A., K. Sameshima, and D. Y. Takahashi. "Generalized partial directed coherence." In *2007 15th International conference on digital signal processing*, pp. 163-166. IEEE, 2007.

43. Lütkepohl, Helmut. *New introduction to multiple time series analysis*. Springer Science & Business Media, 2005.

44. Lütkepohl, Helmut. *Handbook of matrices*. Vol. 1. Chichester: Wiley, 1996.

45. Patnaik, P. B. "The non-central χ^2-and F-distribution and their applications." *Biometrika* 36, no. 1/2 (1949): 202-232.

46. Gubner, John A. *Probability and random processes for electrical and computer engineers*. Cambridge University Press, 2006.

47. Press, William, H., et al. *Numerical recipes 3rd edition: The art of scientific computing*. Cambridge university press, 2007.

48. Moler, Cleve. "Matlab incorporates LAPACK." *Cleve's Corner, MATLAB News&Notes* (2000).

49. Lehoucq, Richard B., Danny C. Sorensen, and Chao Yang. *ARPACK users' guide: solution of large-scale eigenvalue problems with implicitly restarted Arnoldi methods*. Society for Industrial and Applied Mathematics, 1998.

50. Calvetti, Daniela, Lothar Reichel, and Danny Chris Sorensen. "An implicitly restarted Lanczos method for large symmetric eigenvalue problems." *Electronic Transactions on Numerical Analysis* 2, no. 1 (1994): 21.